LOW-CALCIUM FLY ASH-BASED GEOPOLYMER CONCRETE: LONG-TERM PROPERTIES

By

S. E. Wallah and B. V. Rangan

Research Report GC 2
Faculty of Engineering
Curtin University of Technology
Perth, Australia

2006

PREFACE

From 2001, we have conducted some important research on the development, manufacture, behaviour, and applications of Low-Calcium Fly Ash-Based Geopolymer Concrete. This concrete uses no Portland cement; instead, we use the low-calcium fly ash from a local coal burning power station as a source material to make the binder necessary to manufacture concrete.

Concrete usage around the globe is second only to water. An important ingredient in the conventional concrete is the Portland cement. The production of one ton of cement emits approximately one ton of carbon dioxide to the atmosphere. Moreover, cement production is not only highly energy-intensive, next to steel and aluminium, but also consumes significant amount of natural resources. In order to meet infrastructure developments, the usage of concrete is on the increase. Do we build additional cement plants to meet this increase in demand for concrete, or find alternative binders to make concrete?

On the other hand, already huge volumes of fly ash are generated around the world; most of the fly ash is not effectively used, and a large part of it is disposed in landfills. As the need for power increases, the volume of fly ash would increase.

Both the above issues are addressed in our work. We have covered significant area in our work, and developed the know-how to manufacture low-calcium fly ash-based geopolymer concrete. Our research has already been published in more than 30 technical papers in various international venues.

This Research Report describes the long-term properties of low-calcium fly ash-based geopolymer concrete. Earlier, the Research Report GC1 presented the development, the mixture proportions, and the short-term properties of low-calcium fly ash-based geopolymer concrete. A subsequent Research Report GC3 covers the behaviour and strength of reinforced geopolymer concrete structural beams and columns.

Heat-cured low-calcium fly ash-based geopolymer concrete has excellent compressive strength, suffers very little drying shrinkage and low creep, excellent resistance to sulfate attack, and good acid resistance. It can be used in many infrastructure applications. One ton of low-calcium fly ash can be utilised to produce about 2.5 cubic metres of high quality geopolymer concrete, and the bulk price of chemicals needed to manufacture this concrete is cheaper than the bulk price of one ton of Portland cement. Given the fact that fly ash is considered as a waste material, the low-calcium fly ash-based geopolymer concrete is, therefore, cheaper than the Portland cement concrete. The special properties of geopolymer concrete can further enhance the economic benefits. Moreover, reduction of one ton of carbon dioxide yields one carbon credit and, the monetary value of that one credit is approximately 20 Euros. This carbon credit significantly adds to the economy offered by the geopolymer concrete. In all, there is so much to be gained by using geopolymer concrete.

We are happy to participate and assist the industries to take the geopolymer concrete technology to the communities in infrastructure applications. We passionately believe that our work is a small step towards a broad vision to serve the communities for a better future.

For further information, please contact: Professor B. Vijaya Rangan BE PhD FIE Aust FACI, CPEng, Emeritus Professor of Civil Engineering, Faculty of Engineering, Curtin University of Technology, Perth, WA 6845, Australia; Telephone: 61 8 9266 1376, Email: V.Rangan@curtin.edu.au

ACKNOWLEDGEMENTS

The authors are grateful to Emeritus Professor Joseph Davidovits, Director, Geopolymer Institute, Saint-Quentin, France, and to Dr Terry Gourley, Rocla Australia for their advice and encouragement during the conduct of the research.

An Australian Development Scholarship supported the first author. The authors are grateful to Mr. Djwantoro Hardjito and Mr. Dody Sumajouw, the other members of the research team, for their contributions.

The experimental work was carried out in the laboratories of the Faculty of Engineering at Curtin University of Technology. The authors are grateful to the support and assistance provided by the team of talented and dedicated technical staff comprising Mr. Roy Lewis, Mr. John Murray, Mr. Dave Edwards, Mr. Rob Cutter, and Mr. Mike Ellis.

TABLE OF CONTENTS

LIST OF FIGURES

LIST OF TABLES

CHAPTER 1:
INTRODUCTION

1.1 Background

Concrete is one of the most widely used construction materials; it is usually associated with Portland cement as the main component for making concrete. The demand for concrete as a construction material is on the increase. It is estimated that the production of cement will increase from about from 1.5 billion tons in 1995 to 2.2 billion tons in 2010 (Malhotra, 1999).

On the other hand, the climate change due to global warming, one of the greatest environmental issues has become a major concern during the last decade. The global warming is caused by the emission of greenhouse gases, such as CO_2, to the atmosphere by human activities. Among the greenhouse gases, CO_2 contributes about 65% of global warming (McCaffrey, 2002). The cement industry is responsible for about 6% of all CO_2 emissions, because the production of one ton of Portland cement emits approximately one ton of CO_2 into the atmosphere (Davidovits, 1994c; McCaffrey, 2002).

Although the use of Portland cement is still unavoidable until the foreseeable future, many efforts are being made in order to reduce the use of Portland cement in concrete. These efforts include the utilisation of supplementary cementing materials such as fly ash, silica fume, granulated blast furnace slag, rice-husk ash and metakaolin, and finding alternative binders to Portland cement.

In this respect, the geopolymer technology proposed by Davidovits (1988a; 1988b) shows considerable promise for application in concrete industry as an alternative binder to the Portland cement. In terms of reducing the global warming, the geopolymer technology could reduce the CO_2 emission to the atmosphere caused by cement and aggregates industries by about 80% (Davidovits, 1994c).

Inspired by the geopolymer technology and the fact that fly ash is a waste material abundantly available, in 2001, the Geopolymer Concrete Research Group at Curtin

University of Technology commenced a comprehensive research programme on '**Low-Calcium Fly Ash-Based Geopolymer Concrete'.** The first part of this research studied the development of mixture proportions, the manufacture of low-calcium fly ash-based geopolymer concrete, the effect of main parameters on the short-term engineering properties of fresh and hardened concrete (Djwantoro and Rangan 2005).

1.2 Objectives

The objectives of this research therefore are to study the following long-term properties of low-calcium fly ash-based geopolymer concrete:

1. Creep behaviour under sustained load
2. Drying shrinkage behaviour
3. Sulfate resistance
4. Resistance to sulfuric acid

1.3 Scope of the Work

The experimental work involved conduct of long-term tests on low-calcium fly ash-based geopolymer concrete. The tests currently available for Portland cement concrete were used. In the experimental work, only one source of dry low-calcium fly ash (ASTM Class F) from a local power station was used. Analytical methods available for Portland cement concrete were used to predict the test results.

1.4 Organisation of Report

Chapter 2 gives a brief review of geopolymer technology and the past research on geopolymers.

Chapter 3 describes the experimental work including the materials used, mixture proportions, manufacture and curing of the test specimens, test parameters, test procedures and equipment used for the conduct of the tests.

Chapter 4 presents and discusses the experimental results and the analysis of the results.

Chapter 5 summarises and concludes the results of this study.

A list of References and Appendices are given at the end of the Report.

CHAPTER 2:
LITERATURE REVIEW

2.1 Introduction

This Chapter presents a brief review of the terminology and chemistry of geopolymers, and past studies on geopolymers. Additional review of geopolymer technology is available elsewhere (Hardjito and Rangan, 2005).

2.2 Geopolymers

2.2.1 Terminology and Chemistry

The term 'geopolymer' was first introduced by Davidovits in 1978 to describe a family of mineral binders with chemical composition similar to zeolites but with an amorphous microstructure. He also suggested the use of the term 'poly(sialate)' for the chemical designation of geopolymers based on silico-aluminate (Davidovits, 1988a, 1988b, 1991; van Jaarsveld et. al., 2002a); Sialate is an abbreviation for silicon-oxo-aluminate.

Poly(sialates) are chain and ring polymers with Si^{4+} and AL^{3+} in IV-fold coordination with oxygen and range from amorphous to semi-crystalline with the empirical formula:

$$M_n\ (-(SiO_2)_z-AlO_2)_n \cdot wH_2O \qquad (2\text{-}1)$$

where "z" is 1, 2 or 3 or higher up to 32; M is a monovalent cation such as potassium or sodium, and "n" is a degree of polycondensation (Davidovits, 1984, 1988b, 1994b, 1999). Davidovits (1988b; 1991; 1994b; 1999) has also distinguished 3 types of polysialates, namely the Poly(sialate) type (-Si-O-Al-O), the Poly(sialate-siloxo) type (-Si-O-Al-O-Si-O) and the Poly(sialate-disiloxo) type (-Si-O-Al-O-Si-O). The structures of these polysialates can be schematised as in Figure 2.1.

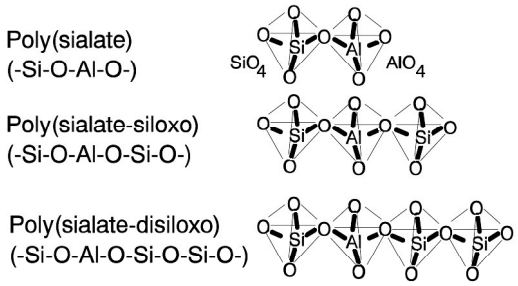

Figure 2.1 Chemical structures of polysialates

Geopolymerization involves the chemical reaction of alumino-silicate oxides (Si_2O_5, Al_2O_2) with alkali polysilicates yielding polymeric Si – O – Al bonds. Polysilicates are generally sodium or potassium silicate supplied by chemical industry or manufactured fine silica powder as a by-product of ferro-silicon metallurgy. Equation 2-2 shows an example of polycondensation by alkali into poly (sialate-siloxo).

$$(Si_2O_5, Al_2O_2)n + nSiO_2 + nH_2O \xrightarrow{NaOH,\ KOH} n(OH)_3\ -Si-O-\overset{(-)}{\underset{|}{Al}}(OH)_2-O-Si-(OH)_3$$

$$n(OH)_3\ -Si-O-\overset{(-)}{\underset{|}{Al}}(OH)_2-O-Si-(OH)_3 \xrightarrow{NaOH,\ KOH} (Na,K)^{(+)} -(-Si-O-\overset{(-)}{Al}-O-Si-O-) + nH_2O$$

(2-2)

Unlike ordinary Portland/pozzolanic cements, geopolymers do not form calcium-silicate-hydrates (CSHs) for matrix formation and strength, but utilise the polycondensation of silica and alumina precursors and a high alkali content to attain structural strength. Therefore, geopolymers are sometimes referred to as alkali-activated alumino silicate binders (Davidovits, 1994a; Palomo et. al., 1999; Roy, 1999; van Jaarsveld et. al., 2002a). However, Davidovits (1999; 2005) stated that using the term 'alkali-activated' could create significant confusion and generate false granted ideas about geopolymer concrete. For example, the use of the term

'alkali-activated cement' or 'alkali-activated fly ash' can be confused with the term 'Alkali-aggregate reaction (AAR)', a harmful property well known in concrete.

The last term of Equation 2-2 indicates that water is released during the chemical reaction that occurs in the formation of geopolymers. This water is expelled from the mixture during the curing process.

2.2.2. Source Materials and Alkaline Liquids

There are two main constituents of geopolymers, namely the source materials and the alkaline liquids. The source materials for geopolymers based on alumino-silicate should be rich in silicon (Si) and aluminium (Al). These could be natural minerals such as kaolinite, clays, micas, andalousite, spinel, etc whose empirical formula contains Si, Al, and oxygen (O) (Davidovits, 1988c). Alternatively, by-product materials such as fly ash, silica fume, slag, rice-husk ash, red mud, etc could be used as source materials. The choice of the source materials for making geopolymers depends on factors such as availability, cost, and type of application and specific demand of the end users. The alkaline liquids are from soluble alkali metals that are usually Sodium or Potassium based.

Since 1972, Davidovits (1988c; 1988d) worked with kaolinite source material with alkalis (NaOH, KOH) to produce geopolymers. The technology for making the geopolmers has been disclosed in various patents issued on the applications of the so-called "SILIFACE-Process". Later, Davidovits (1999) also introduced a pure calcined kaolinite called KANDOXI (**KA**olinite, **N**acrite, **D**ickite **OXI**de) which is calcined for 6 hours at 750^{o}C. This calcined kaolinite like other calcined materials performed better in making geopolymers compared to the natural ones.

Xu and Van Deventer (1999; 2000) have also studied a wide range of alumino-silicate minerals to make geopolymers. Their study involved sixteen natural Si-Al minerals which covered the ring, chain, sheet, and framework crystal structure groups, as well as the garnet, mica, clay, feldspar, sodalite and zeolite mineral groups. It was found that a wide range of natural alumino-silicate minerals provided potential sources for synthesis of geopolymers. For alkaline solutions, they used

sodium or potassium hydroxide. The test results have shown that potassium hydroxide (KOH) gave better results in terms of the compressive strength and the extent of dissolution.

Among the waste or by-product materials, fly ash and slag are the most potential source of geopolymers. Several studies have been reported related to the use of these source materials. Cheng and Chiu (2003) reported the study of making fire-resistant geopolymer using granulated blast furnace slag combined with metakaolinite. The combination of potassium hydroxide and sodium silicate was used as alkaline liquids. Van Jaarsveld et. al., (1997; 1999) identified the potential use of waste materials such as fly ash, contaminated soil, mine tailings and building waste to immobilise toxic metals. Palomo et. al., (1999) reported the study of fly ash-based geopolymers. They used combinations of sodium hydroxide with sodium silicate and potassium hydroxide with potassium silicate as alkaline liquids. It was found that the type of alkaline liquid is a significant factor affecting the mechanical strength, and that the combination of sodium silicate and sodium hydroxide gave the highest compressive strength.

Van Jaarsveld et. al. (2003) reported that the particle size, calcium content, alkali metal content, amorphous content, and morphology and origin of the fly ash affected the properties of geopolymers. It was also revealed that the calcium content in fly ash played a significant role in strength development and final compressive strength as the higher the calcium content resulted in faster strength development and higher compressive strength. However, in order to obtain the optimal binding properties of the material, fly ash as a source material should have low calcium content and other characteristics such as unburned material lower than 5%, Fe_2O_3 content not higher than 10%, 40-50% of reactive silica content, 80-90% particles with size lower than 45 μm and high content of vitreous phase (Fernández-Jiménez & Palomo, 2003). Gourley (2003) also stated that the presence of calcium in fly ash in significant quantities could interfere with the polymerisation setting rate and alters the microstructure. Therefore, it appears that the use of Low Calcium (ASTM Class F) fly ash is more preferable than High Calcium (ASTM Class C) fly ash as a source material to make geopolymers.

Swanepoel and Strydom (2002), Phair and Van Deventer (2001; 2002), Van Jaarsveld (2002a; 2002b) and Bakharev (2005a; 2005b; 2005c) also presented studies on fly ash as the source material to make geopolymers. Davidovits (2005) reported results of his preliminary study on fly ash-based geopolymer as a part of a EU sponsored project entitled 'Understanding and mastering coal fired ashes geopolymerisation process in order turn potential into profit', known under the acronym of GEOASH.

Every source material has advantages and disadvantages. For example, metokaolin as a source material has high dissolvability in the reactant solution, produces a controlled Si/Al ratio in the geopolymer, and is white in colour (Gourley, 2003). However, metakaolin is expensive to produce in large volumes because it has to be calcined at temperatures around 500^{o}C – 700^{o}C for few hours. In this respect using waste materials such as fly ash is economically advantageous.

2.2.3. Fields of Applications

According to Davidovits (1988b), geopolymeric materials have a wide range of applications in the field of industries such as in the automobile and aerospace, non-ferrous foundries and metallurgy, civil engineering and plastic industries. The type of application of geopolymeric materials is determined by the chemical structure in terms of the atomic ratio Si:Al in the polysialate. Davidovits (1999) classified the type of application according to the Si:Al ratio as presented in Table 2.1. A low ratio of Si:Al of 1, 2, or 3 initiates a 3D-Network that is very rigid, while Si:Al ratio higher than 15 provides a polymeric character to the geopolymeric material. It can be seen from Table 2.1 that for many applications in the civil engineering field a low Si:Al ratio is suitable.

One of the potential fields of application of geopolymeric materials is in toxic waste management because geopolymers behave similar to zeolitic materials that have been known for their ability to absorb the toxic chemical wastes (Davidovits, 1988b). Comrie et. al., (1988) also provided an overview and relevant test results of the potential of the use of geopolymer technology in toxic waste management. Based on tests using GEOPOLYMITE 50, they recommend that geopolymeric materials could

be used in waste containment. GEOPOLYMITE 50 is a registered trademark of Cordi-Geopolymere SA, a type of geopolymeric binder prepared by mixing various alumina-silicates precondensates with alkali hardeners (Davidovits, 1988b).

Table 2.1 Applications of Geopolymeric Materials Based on Si:Al Atomic Ratio

Si:Al ratio	Applications
1	- Bricks - Ceramics - Fire protection
2	- Low CO_2 cements and concretes - Radioactive and toxic waste encapsulation
3	- Fire protection fibre glass composite - Foundry equipments - Heat resistant composites, 200^{o}C to 1000^{o}C - Tooling for aeronautics titanium process
>3	- Sealants for industry, 200^{o}C to 600^{o}C - Tooling for aeronautics SPF aluminium
20 - 35	- Fire resistant and heat resistant fibre composites

Another application of geopolymer is in the strengthening of concrete structural elements. Balaguru et. al. (1997) reported the results of the investigation on using geopolymers, instead of organic polymers, for fastening carbon fabrics to surfaces of reinforced concrete beams. It was found that geopolymer provided excellent adhesion to both concrete surface and in the interlaminar of fabrics. In addition, the researchers observed that geopolymer was fire resistant, did not degrade under UV light, and was chemically compatible with concrete.

In Australia, the geopolymer technology has been used to develop sewer pipeline products, railway sleepers, building products including fire and chemically resistant wall panels, masonry units, protective coatings and repairs materials, shotcrete and high performance fibre reinforced laminates (Gourley, 2003; Gourley & Johnson, 2005).

2.2.4. Properties of Geopolymers

Previous studies have reported that geopolymers possess high early strength, low shrinkage, freeze-thaw resistance, sulfate resistance, corrosion resistance, acid resistance, fire resistance, and no dangerous alkali-aggregate reaction.

Based on laboratory tests, Davidovits (1988b) reported that geopolymer cement can harden rapidly at room temperature and gain the compressive strength in the range of 20 MPa after only 4 hours at 20^{o}C and about 70-100 MPa after 28 days. Comrie et. al., (1988) conducted tests on geopolymer mortars and reported that most of the 28-day strength was gained during the first 2 days of curing.

Geopolymeric cement was superior to Portland cement in terms of heat and fire resistance, as the Portland cement experienced a rapid deterioration in compressive strength at 300^{o}C, whereas the geopolymeric cements were stable up to 600^{o}C (Davidovits, 1988b; 1994b). It has also been shown that compared to Portland cement, geopolymeric cement has extremely low shrinkage.

The presence of alkalis in the normal Portland cement or concrete could generate dangerous Alkali-Aggregate-Reaction. However the geopolymeric system is safe from that phenomenon even with higher alkali content. As demonstrated by Davidovits (1994a; 1994b), based on ASTM C227 bar expansion test, geopolymer cements with much higher alkali content compared to Portland cement did not generate any dangerous alkali-aggregate reaction where the Portland cement did.

Geopolymer cement is also acid-resistant, because unlike the Portland cement, geopolymer cements do not rely on lime and are not dissolved by acidic solutions. As shown by the tests of exposing the specimens in 5% of sulfuric acid and chloric acid, geopolymer cements were relatively stable with the weight lose in the range of 5-8% while the Portland based cements were destroyed and the calcium alumina cement lost weight about 30-60% (Davidovits, 1994b). Some recently published papers (Bakharev, 2005c; Gourley & Johnson, 2005; Song et. al., 2005a) also reported the results of the tests on acid resistance of geopolymers and geopolymer concrete. By observing the weight loss after acid exposure, these researchers concluded that

geopolymers or geopolymer concrete is superior to Portland cement concrete in terms of acid resistance as the weight loss is much lower. However, Bakharev and Song et. al has also observed that there is degradation in the compressive strength of test specimens after acid exposure and the rate of degradation depended on the period of exposure. Tests conducted by U.S. Army Corps of Engineers also revealed that geopolymers have superior resistance to chemical attack and freeze/thaw, and very low shrinkage coefficients (Comrie et. al., 1988; Malone et. al., 1985).

CHAPTER 3:
EXPERIMENTAL WORK

3.1. Introduction

This Chapter describes the experimental work. First, the materials, mixture proportions, manufacturing and curing of the test specimens are explained. This is then followed by description of types of specimens used, test parameters, and test procedures.

3.2. Materials

The materials used for making fly ash-based geopolymer concrete specimens are low-calcium dry fly ash as the source material, aggregates, alkaline liquids, water, and super plasticiser.

3.2.1. Fly Ash

Fly ash used in this study was low-calcium (ASTM Class F) dry fly ash from Collie Power Station, Western Australia. Three batches of fly ash were obtained during the period of this study from 2002 to 2005.

The chemical composition of the three batches of the fly ash, given in Table 3.1, was determined by X-Ray Fluorescence (XRF) analysis. As can be seen from Table 3.1 that, for all batches of fly ash, the silicon and aluminium constitute about 80% of the total mass and the ratio of silicon to aluminium oxide is about 2.

The particle size distribution of the fly ash is presented in Figures 3.1, 3.2 and 3.3 for Batch-1, Batch-2 and Batch-3 respectively. From the analysis of these data, it was found that the specific surface area of the fly ash was 1.29 m^2/cc,1.94 m^2/cc and 1.52 m^2/cc for Batch-1, Batch-2, and Batch-3 respectively. In these Figures, Graph A shows the percentage of the volume passing and Graph B shows the percentage volume for certain sizes. For Batch-1 fly ash, 80% of the particles were smaller than 55 μm, while for Batch-2 and Batch-3, this number was 39 μm and 46 μm respectively.

Table 3.1 Chemical Composition of Fly Ash (% by mass)

Oxides	Batch-1	Batch-2	Batch-3
SiO_2	53.36	47.80	48.0
Al_2O_3	26.49	23.40	29.0
Fe_2O_3	10.86	17.40	12.7
CaO	1.34	2.42	1.78
Na_2O	0.37	0.31	0.39
K_2O	0.80	0.55	0.55
TiO_2	1.47	1.328	1.67
MgO	0.77	1.19	0.89
P_2O_5	1.43	2.00	1.69
SO_3	1.70	0.29	0.5
Cr	0.00	0.01	0.016
MnO	0.00	0.12	0.06
Ba	0.00	0.00	0.28
Sr	0.00	0.00	0.25
V	0.00	0.00	0.017
ZrO_2	0.00	0.00	0.06
LOI*	1.39	1.10	1.61

*Loss on ignition

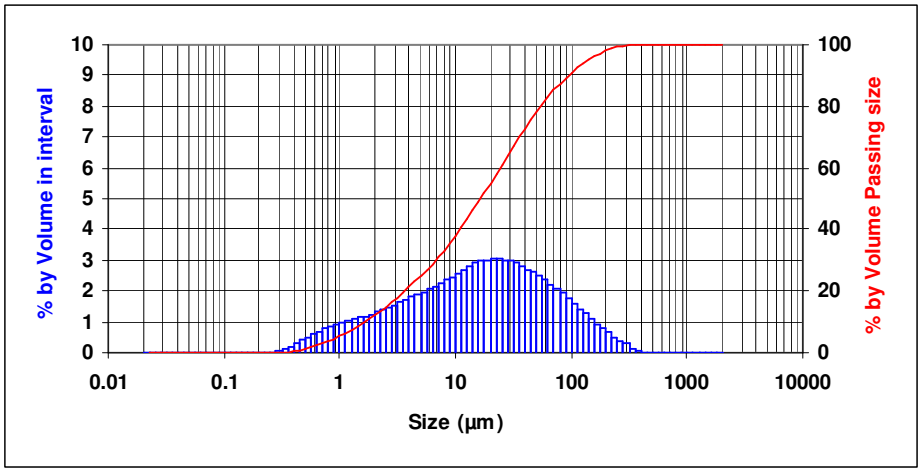

Figure 3.1 Particle Size Distribution of Batch-1 Fly Ash

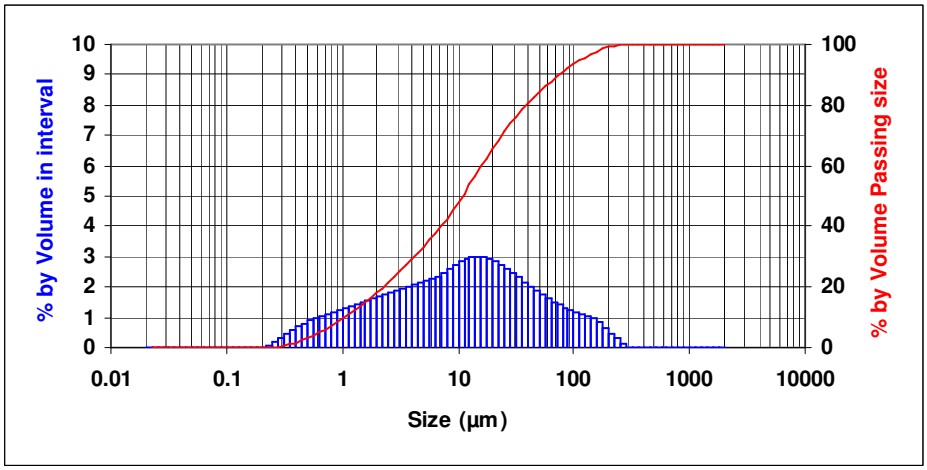

Figure 3.2 Particle Size Distribution of Batch-2 Fly Ash

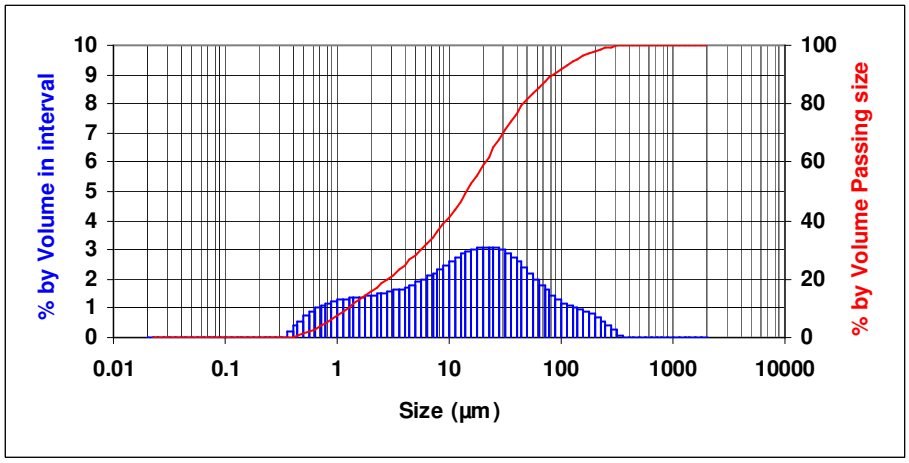

Figure 3.3 Particle Size Distribution of Batch-3 Fly Ash

3.2.2. Aggregates

Local aggregates, comprising 20 mm, 14 mm and 7 mm coarse aggregates and fine aggregates, in saturated surface dry condition, were used. The coarse aggregates were crushed granite-type aggregates and the fine aggregate was fine sand. The fineness modulus of combined aggregates was 5.0. The grading of the aggregates is as presented in Table 3.2.

Table 3.2 Grading of Combined Aggregates

Sieve Size	Aggregates				Combination *)	BS 882:92
	20 mm	14 mm	7 mm	Fine		
19.00 mm	93.34	99.99	100.00	100.00	99.00	95-100
9.50 mm	3.89	17.40	99.90	100.00	69.03	
3.75 mm	0.90	2.99	20.10	100.00	37.77	35-55
2.36 mm	0.88	1.07	3.66	100.00	31.63	
1.18 mm	0.87	0.81	2.05	99.99	31.01	
600 µm	0.85	0.70	1.52	79.58	23.67	10-35
300 µm	0.75	0.59	1.08	16.53	5.57	
150 µm	0.54	0.42	0.62	1.11	0.72	0-8

*) 15% (20 mm) + 20% (14 mm) + 35% (7 mm) + 30% (Fine)

3.2.3. Alkaline Liquid

The alkaline liquid used was a combination of sodium silicate solution and sodium hydroxide solution. The sodium silicate solution (Na_2O= 13.7%, SiO_2=29.4%, and water=55.9% by mass) was purchased from a local supplier in bulk. The sodium hydroxide (NaOH) in flakes or pellets from with 97%-98% purity was also purchased from a local supplier in bulk. The NaOH solids were dissolved in water to make the solution.

3.2.4. Super Plasticiser

In order to improve the workability of fresh concrete, high-range water-reducing naphthalene based super plasticiser was added to the mixture.

3.3. Mixture Proportions

An extensive study on the development and the manufacture of low-calcium fly ash-based geopolymer concrete has been in progress at Curtin when the present research was undertaken. Some results of that study have already been reported in several publications (Hardjito et. al., 2002a; Hardjito et. al., 2003, 2004a, 2004b, 2005a, 2005b; Rangan et. al., 2005a, 2005b). Complete details of that study are available in a Research Report by Hardjito and Rangan (2005). Based on that study, two different

mixture proportions were formulated for making concrete specimens and one mixture proportion for mortar specimens.

The mixture proportions per m^3 for concrete are given in Table 3.3, while Table 3.4 presents the mixture proportion for mortar. Note that there were only two differences between the concrete Mixture-1 and Mixture-2 (Table 3.3). In Mixture-1, the concentration of the sodium hydroxide solution was 8 Molars (M), and there was no extra added water. In Mixture-2, the concentration of the sodium hydroxide solution was 14 Molars (M), and the mixture contained extra added water. These two mixture proportions were selected to yield two different concrete compressive strengths. The mixture proportion for mortar was selected based on concrete Mixture-1, by removing the coarse aggregates from the composition and adjusting the mass of the remaining elements so that the relative proportions of the elements remained approximately similar to that of concrete Mixture-1.

Table 3.3 Concrete Mixture Proportions

Materials		Mass (kg/m^3)	
		Mixture-1	Mixture-2
Coarse aggregates:	20 mm	277	277
	14 mm	370	370
	7 mm	647	647
Fine sand		554	554
Fly ash (low-calcium ASTM Class F)		408	408
Sodium silicate solution(SiO_2/Na_2O=2)		103	103
Sodium hydroxide solution		41 (8M)	41 (14M)
Super Plasticiser		6	6
Extra water		0	22.5

Table 3.4 Mortar Mixture Proportion

Materials	Mass (kg/m^3)
Fine sand	1052
Fly ash (low-calcium ASTM Class F)	774
Sodium silicate solution (SiO_2/Na_2O=2)	196
Sodium hydroxide solution (8M)	78
Super Plasticiser	12

3.4. Manufacture of Test Specimens

3.4.1. Preparation of Liquids

The sodium hydroxide (NaOH) solids were dissolved in water to make the solution. The mass of NaOH solids in a solution varied depending on the concentration of the solution expressed in terms of molar, M. For instance, NaOH solution with a concentration of 8M consisted of 8x40 = 320 grams of NaOH solids (in flake or pellet form) per litre of the solution, where 40 is the molecular weight of NaOH. The mass of NaOH solids was measured as 262 grams per kg of NaOH solution of 8M concentration. Similarly, the mass of NaOH solids per kg of the solution for 14M concentration was measured as 404 grams. Note that the mass of NaOH solids was only a fraction of the mass of the NaOH solution, and water was the major component.

The sodium silicate solution and the sodium hydroxide solution were mixed together at least one day prior to use to prepare the alkaline liquid. On the day of casting of the specimens, the alkaline liquid was mixed together with the super plasticizer and the extra water (if any) to prepare the liquid component of the mixture.

3.4.2. Manufacture of Fresh Concrete and Casting

The fly ash and the aggregates were first mixed together in the 80-litre capacity laboratory concrete pan mixer for about 3 minutes. The liquid component of the mixture was then added to the dry materials and the mixing continued for further about 4 minutes to manufacture the fresh concrete (Figure 3.4).

The fresh concrete was cast into the moulds immediately after mixing, in three layers for cylindrical specimens and two layers for prismatic specimens. For compaction of the specimens, each layer was given 60 to 80 manual strokes using a rodding bar, and then vibrated for 12 to 15 seconds on a vibrating table (Figure 3.5).

Figure 3.4 Fresh Geopolymer Concrete

Figure 3.5 Compaction of Concrete Specimens

Before the fresh concrete was cast into the moulds, the slump value of the fresh concrete was measured as shown in Figure 3.6.

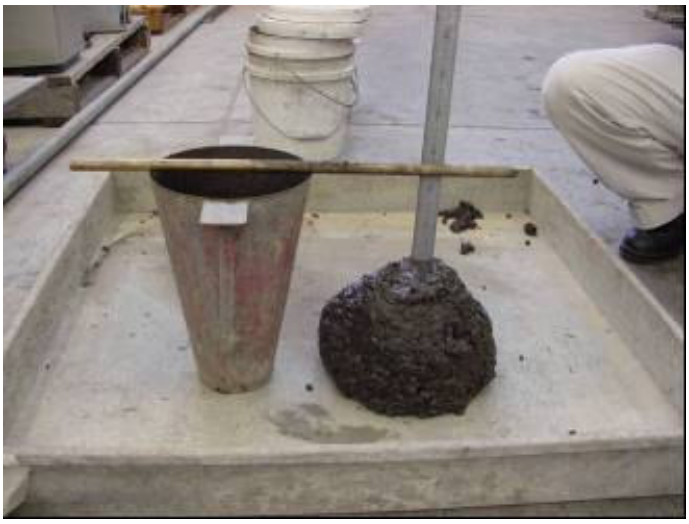

Figure 3.6 Measurement of Slump

3.4.3. Manufacture of Fresh Mortar and Casting

The fly ash and the fine sand were first mixed together in a Hobart mixer for about 3 minutes. The liquid component of the mixture was then added to the dry materials and the mixing continued for further about 4 minutes to manufacture the fresh mortar (Figure 3.7). The fresh mortar was cast into the moulds immediately after mixing and compacted by vibrating the moulds for 20 seconds on a vibrating table (Figure 3.8).

Figure 3.7 Fresh Geopolymer Mortar

Figure 3.8 Compaction of Mortar Specimens

3.5. Curing Of Test Specimens

After casting, the test specimens were covered with vacuum bagging film to minimise the water evaporation during curing at an elevated temperature. Two types of heat curing were used in this study, i.e. dry curing and steam curing. For dry curing, the test specimens were cured in the oven (Figure 3.9) and for steam curing, they were cured in the steam curing chamber (Figure 3.10). Based on Curtin studies, the specimens were heat-cured at 60^{o}C for 24 hours (Hardjito et. al., 2002a, 2002b; Hardjito et. al., 2003, 2004a, 2004b; Hardjito & Rangan, 2005; Hardjito et. al., 2005a, 2005b; Rangan et. al., 2005a, 2005b).

After the curing period, the test specimens were left in the moulds for at least six hours in order to avoid a drastic change in the environmental conditions. After demoulding, the specimens were left to air-dry in the laboratory until the day of test.

Some series of specimens were not heat-cured, but left in ambient conditions at room temperature in the laboratory.

Figure 3.9 Dry (oven) Curing

Figure 3.10 Steam Curing

3.6. Compressive Strength Test

For each series of tests, a set of standard size cylinders were made. The size of cylinders was either 100 mm diameter by 200 mm high or 150 mm diameter by 300 mm high depending on the type of test. The cylinders were tested in compression in accordance with the test procedures given in the Australian Standard, AS 1012.9-1999, Methods of Testing Concrete – Determination of the compressive strength of concrete specimens (1999).

3.7. Creep Test

3.7.1. Test Specimens

Test specimens for the creep test were 150x300 mm cylinders as shown in Figure 3.11. Eight cylinders were prepared for each test. Three cylinders were used for measuring the creep, two companion cylinders measured the drying shrinkage and the other three cylinders were used for the compressive strength test.

Figure 3.11 Creep Test Specimens

3.7.2. Test Parameters

Creep strains were measured for two geopolymer concrete mixtures, Mixture-1 and Mixture-2 as given in Table 3.3. Two types of curing, namely, dry curing and steam curing, were used. The test parameters for creep test are summarised in Table 3.5.

Table 3.5 Test Parameters for Creep Test

Test Designation	Mixture	Curing type
1CR	Mixture-1	Dry
2CR	Mixture-1	Steam
3CR	Mixture-2	Dry
4CR	Mixture-2	Steam

3.7.3. Test Procedure

The creep tests were performed in accordance with the Australian Standard, AS 1012.16-1996, Methods of Testing Concrete – Determination of creep of concrete cylinders in compression (1996a). The sustained load was applied on the 7^{th} day after casting of the specimens.

3.7.3.1. Strain Measuring Device and Reference Gauge Points

Prior to the commencement of the test, the creep specimens and the companion shrinkage specimens were attached with demec gauge points as shown in Figure 3.12.

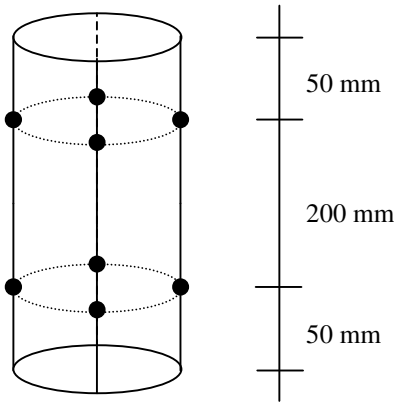

Figure 3.12 Location of Demec Gauge Points on Test Cylinders

3.7.3.2 Test Set up and Measurement

The three specimens for creep test were placed in a specially-built creep testing frame with a hydraulic loading system as shown in Figure 3.13. Before the creep specimens were loaded, the 7-th day compressive strength of geopolymer concrete was determined by testing the three cylinders reserved for the compressive strength test. The creep specimens were applied with a load corresponding to 40 percent of the measured mean compressive strength of concrete. This load was maintained as the sustained load throughout the duration of the test. The strain values were measured and recorded immediately before and after the loading. Strains experienced by the control shrinkage specimens were measured at the same time as the strain measurements on creep specimens. The strain values were measured and recorded at 2 hours, 6 hours, and then every day for the first week, after loading. The measurements then continued once a week until the fourth week. After that, the measurements were done once in 2 weeks until the twelfth week and the once every four weeks until one year. Figure 3.14 shows the creep test in progress.

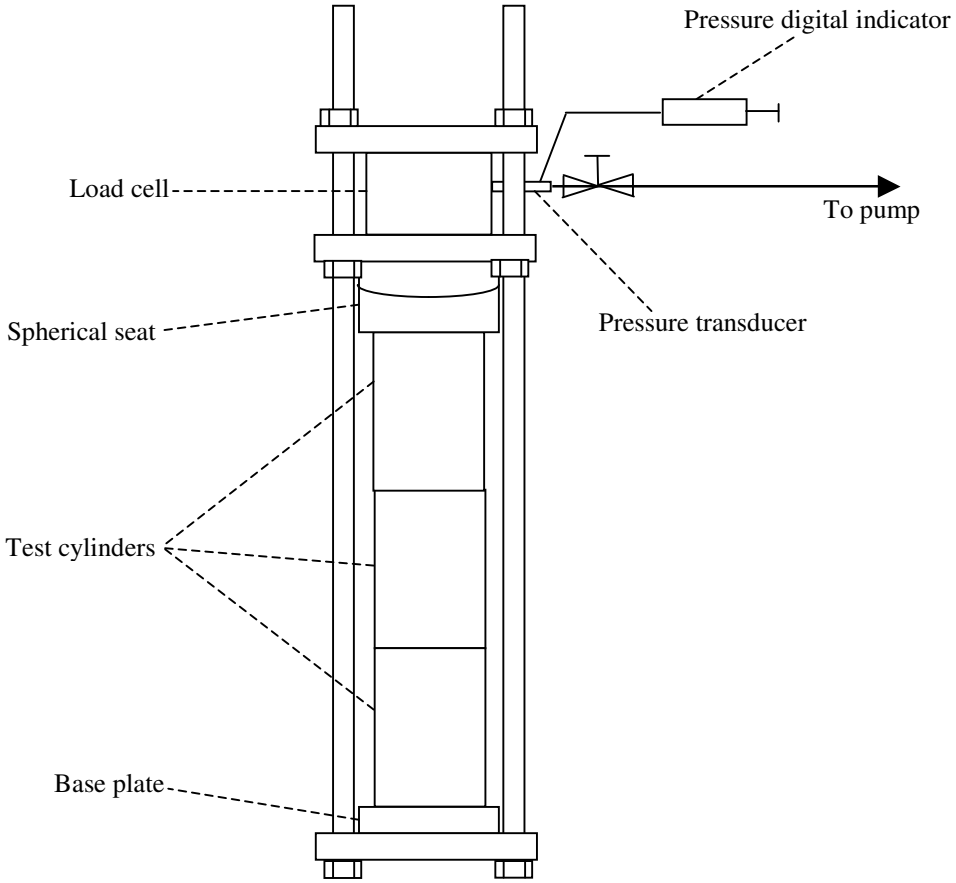

Figure 3.13 Creep Test Set-up

Figure 3.14 Creep Test

The creep tests were conducted in a laboratory room where the temperature was maintained at about 23^{o}C, but the relative humidity could not be controlled. The relative humidity varied between 40% and 60% during the test.

3.8. Drying Shrinkage Test

3.8.1. Test Specimens

Test specimens for drying shrinkage test were 75x75x285 mm prisms with the gauge studs as shown in Figure 3.15. Three specimens were prepared for each type of test. In addition, for each type of test, four 100x200 mm cylindrical specimens were also prepared for compressive strength test.

Figure 3.15 Specimens for Drying Shrinkage Test

3.8.2. Test parameters

As for the creep test, Mixture-1 and Mixture-2 (Table 3.2) were also used for drying shrinkage test. Two types of curing were used for each Mixture. The test parameters for the drying shrinkage test are given in Table 3.6.

Table 3.6 Test Parameters for Drying Shrinkage Test

Test Designation	Mixture	Curing type
1DS	Mixture-1	Dry
2DS	Mixture-1	Steam
3DS	Mixture-2	Dry
4DS	Mixture-2	Steam
5DS	Mixture-1	Heat-cured versus Ambient-cured

3.8.3. Test Procedure

The procedure for drying shrinkage test is based on the Australian Standard, AS 1012.13-1992, Methods of Testing Concrete – Determination of the drying shrinkage of concrete for samples prepared in the field or in the laboratory (1992). The shrinkage strain measurements started on the third day after casting the concrete. On the third day after casting, the specimens were demoulded and the first measurement was taken. Horizontal length comparator (Figure 3.16) was used for length measurements. The next measurement was on the fourth day of casting, considered as Day 1 for the drying shrinkage measurements. The measurements then continued every day in the first week, once a week until the fourth week, once in two weeks until the twelfth week, and then once in four weeks until one year.

During the drying shrinkage tests, the specimens were kept in a laboratory room where the temperature was maintained at approximately at 23^{o}C. The relative humidity of the room varied between 40% and 60%.

Figure 3.16 Horizontal Length Comparator with Drying Shrinkage Test Specimen

3.9. Sulfate Resistance Test

3.9.1. Test Specimens

Test specimens for compressive strength and change in mass test were 100x200 mm cylinders, whereas for change in length test the specimens were 75x75x285 mm prisms (Figure 3.17). Four specimens were prepared for each compressive strength and change in mass test, while three specimens were prepared for each change in length test.

Figure 3.17 Specimens for Sulfate Resistance Test

3.9.2. Test parameters

The sulphate resistance of geopolymer concrete was evaluated by measuring the residual compressive strength, change in mass, and change in length after sulfate exposure. The test parameters for sulphate resistance test are presented in Table 3.7. Only Mixture-1(Table 3.3) was used and the test specimens were dry cured at 60^{o}C for 24 hours.

Table 3.7. Test Parameters for Sulfate Resistance Test

Parameter to study	Specimens	Test Condition of Specimen	Exposure period (weeks)
Change in compressive strength	Cylinder 100x200 mm	SSD*	1, 4, 8, 12, 24, 36, 52
		Dry	
Change in length	Prism 75x75x285 mm	SSD*	Up to 52 weeks (1 year)
Change in mass	Cylinder 100x200 mm	SSD*	Up to 52 weeks (1 year)

* Saturated-surface-dry

3.9.3. Test Procedure

The test procedure for sulfate resistance test was developed by modifying the related Standards for normal Portland cement and concrete (Standards-ASTM, 1993, 1995, 1997; Standards-Australia, 1996b). The test specimens were immersed in sulfate solution on the 7th day after casting.

3.9.3.1. Sulfate Solution

Sodium sulfate (Na_2SO_4) solution with 5% concentration was used as the standard exposure solution for all tests. The specimens were immersed in the sulfate solution in a container (Figure 3.18); the volume proportion of sulfate solution to specimens

was four to one. In order to maintain the concentration, the solution was replaced every month.

Figure 3.18 Specimens Soaked in Sodium Sulfate Solution

3.9.3.2. Change in Compressive Strength

The change in compressive strength after sulfate exposure was determined by testing the compressive strength of the specimens after selected periods of exposure. The specimens were tested either in SSD (saturated-surface-dry) condition or in dry condition. For the SSD condition, the specimens were removed from the sulphate solution, wiped clean, and then tested immediately in compression. For the dry condition, the specimens were removed from the sulphate solution, left to air-dry for a week in the laboratory ambient condition, and then loaded in compression.

3.9.3.3. Change in Mass

Change in mass of specimens was measured after selected periods of exposure up to one year. On the day the mass was measured, the specimens were removed from the sulphate solution, and wiped clean prior to the measurement. Mass measurements were done using a laboratory scale. The specimens were returned to the sulphate solution container immediately after the measurement was done.

3.9.3.4. Change in Length

The specimens used for change in length test were 75x75x285 mm prisms with gauge studs, similar to those used for drying shrinkage tests as described in Section 3.8. Change in length of the specimens after sulfate exposure was measured for the selected periods up to one year. Prior to the measurements, the specimens were removed form the sulphate solution, and wiped clean. Immediately after the measurement finished, the specimens were returned to the sulphate solution container. Horizontal Length Comparator (Fig. 3.16) was used to measure the change in length of the specimens.

3.10. Acid Resistance Test

Acid resistance test was conducted on geopolymer concrete and geopolymer mortar. Because no universal or widely accepted standard procedures for acid resistance test exist, the type and concentration of the acid solution to which the specimens were exposed varied. Sulfuric acid is one type of acid solution that is frequently used to simulate the acid attack in sewer pipe systems. In such systems, sulfuric acid attack is a particular problem as it is generated bacterially from hydrogen sulfide. To test the acid resistance of geopolymer concrete, Hime (2003) suggested that the specimens be exposed to sulfuric acid solution with a concentration of pH = 1. This value of pH was also used by Gourley & Johnson (2005) to simulate the acid attack on sewer pipes. Mehta (1985) and Li and Zhao (2003) used 1% and 2% sulfuric acid concentration to simulate the sulfuric acid attack on concrete. Based on those past studies, to evaluate the acid resistance of fly ash-based geopolymer concrete, the specimens were soaked in sulfuric acid solution with selected concentrations ranging from 0.25% to 2% with the measured pH ranges from about 0.9 to 2.1, up to one year of exposure. The test specimens were immersed in sulfuric acid solution in a container; the ratio of the volume of the acid solution to the volume of the specimens was 4. The solution was stirred every week and replaced every month. The acid resistance of geopolymer concrete and geopolymer mortar was then evaluated based on the change in compressive strength and the change in mass after acid exposure.

3.10.1. Tests on Geopolymer Concrete

The test specimens for acid resistance test on geopolymer concrete were 100x200 mm cylinders for both the compressive strength test and the change in mass test. The test parameters are summarised in Table 3.8. Mixture-1 (Table 3.3) was used for all tests and the specimens were dry cured at 60^{o}C for 24 hours.

Table 3.8 Test Parameters of Acid Resistance Test on Geopolymer Concrete

Parameters to study	Specimens	Concentration of acid solution	Exposure period (weeks)
Residual compressive strength	Cylinder 100x200 mm	0.5%	1, 4, 12, 24 & 52
		1%	
		2%	
Change in mass	Cylinder 100x200 mm	2%	Up to 52 weeks (1 year)

For compressive strength test, the specimens were tested in saturated-surface-dry (SSD) condition. On the day of test, the specimens were removed from the acid solution container and wiped clean before testing. Specimens for change in mass test were also removed from the acid solution container and wiped clean prior to the measurement. Immediately after mass measurement using a laboratory scale, the specimens were returned to the acid solution container.

3.10.2. Tests on Geopolymer Mortar

The test specimens for acid resistance test on geopolymer mortar were 75 mm cubes for both compressive strength test and change in mass test. Table 3.9 gives the test parameters for acid resistance test on mortar.

The mixture proportion of geopolymer mortar is given in Table 3.4. As for concrete, the specimens were dry cured at 60^{o}C for 24 hours. Test procedures were the same as for the geopolymer concrete as described in Section 3.10.1.

Table 3.9 Test Parameters of Acid Resistance Test on Geopolymer Mortar

Parameters to study	Specimens	Concentration of acid solution	Exposure period (weeks)
Residual compressive strength	Cube 75 mm	0.25%	1, 4, 12, 24 & 52
		0.5%	
		1%	
Change in mass	Cube 75 mm	1%	Up to 52 weeks (1 year)

CHAPTER 4:
PRESENTATION AND DISCUSSION OF EXPERIMENTAL RESULTS

4.1. Introduction

In this Chapter, the test results are presented and discussed. The test results cover the effect of age on the compressive strength and unit-weight, and the long-term properties of low-calcium fly ash-based geopolymer concrete. The long-term properties include creep under sustained load, drying shrinkage, sulphate resistance, and resistance to sulphuric acid.

Test specimens were made using geopolymer concrete Mixture-1 and Mixture-2, and the geopolymer mortar. The details of these mixtures, the manufacturing process, and the test details are given in Chapter 3.

Each test result plotted in the Figures or given in the Tables is the mean value of results obtained from at least three specimens.

4.2. Compressive Strength and Unit Weight

4.2.1 Mean Compressive Strength and Unit Weight

For each batch of geopolymer concrete made in this study, 100x200 mm cylinders specimens were prepared. At least three of these cylinders were tested for compressive strength at an age of seven days after casting. The unit weight of specimens was also determined at the same time. For these numerous specimens made from Mixture-1 and Mixture-2 and cured at 60^{o}C for 24 hours, the average results are presented in Table 4.1.

Table 4.1. Mean Compressive Strength and Unit Weight

Mixture	Curing type	Compressive strength (MPa)		Unit weight (kg/m^3)	
		Average	Standard Deviation	Average	Standard Deviation
Mixture-1	Dry curing (oven)	58	6	2379	17
	Steam curing	56	3	2388	15
Mixture-2	Dry curing (oven)	45	7	2302	52
	Steam curing	36	8	2302	49

4.2.2. Effect of Age on Compressive Strength and Unit Weight

In order to study the effect of age on compressive strength and unit weight, 100x200 mm cylinders were made from several batches of Mixture-1. The specimens were cured in the oven (dry curing) for 24 hours at 60^{o}C. The test results are presented in Figure 4.1 and Figure 4.2.

Figure 4.1 presents the ratio of the compressive strength of specimens at a particular age as compared to the compressive strength of specimens from the same batch of geopolymer concrete tested on the 7th day after casting. These test data show that the compressive strength increases with age in the order of 10 to 20 percent when compared to the 7th day compressive strength.

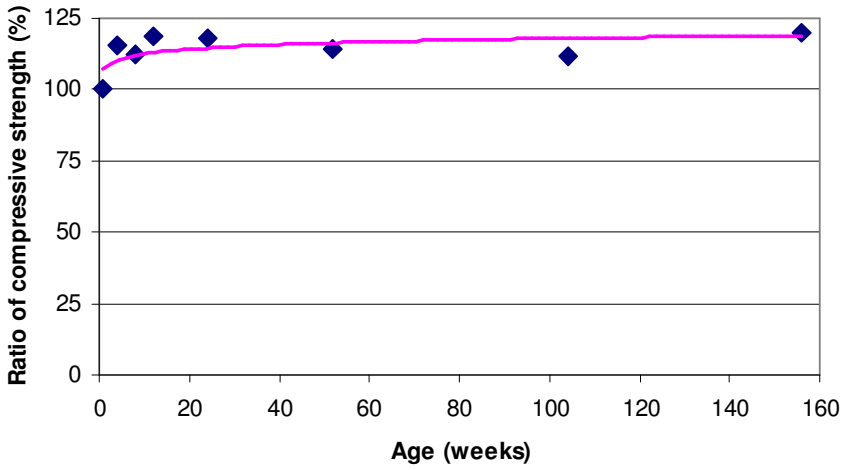

Figure 4.1 Change in Compressive Strength of Heat-cured Geopolymer Concrete with Age

Figure 4.2 presents the change in unit weight of concrete specimens left in the laboratory at room temperature as a percentage of the value at one week after casting. The unit weight of geopolymer concrete decreased slightly in the order of about 2 percent in the first few weeks but remained almost constant after that.

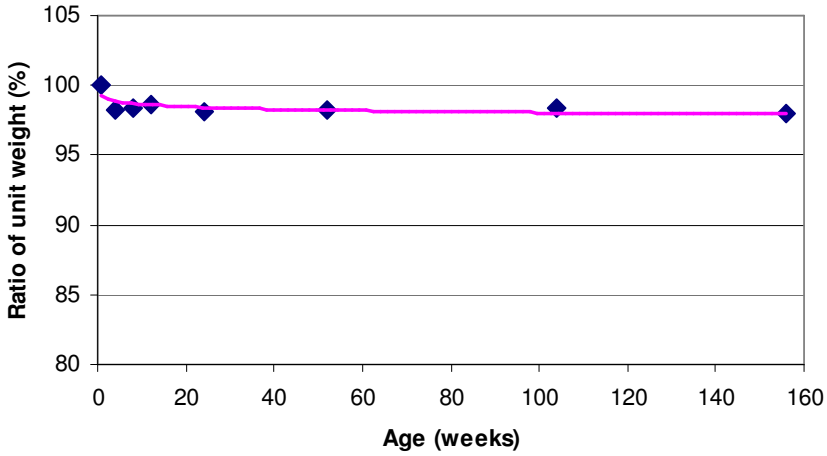

Figure 4.2 Change in Unit Weight of Heat-cured Geopolymer Concrete with Age

The test data shown in Figure 4.1 and Figure 4.2 demonstrate the long-term stability of low-calcium fly ash-based geopolymer concrete.

4.2.3. Compressive Strength of Specimens Cured at Ambient Conditions

In order to study the effect of curing in ambient conditions on the compressive strength of fly ash-based geopolymer concrete, three batches of geopolymer concrete were made using Mixture-1. The test specimens were 100x200 mm cylinders. The first batch, called May 05, was cast in the month of May 2005, while the second batch (July 05) was cast in the month of July 2005 and the third batch (September 05) in September 2005. The ambient temperature in May 2005 during the first week after casting the concrete ranged from about 18 to 25^{o}C, while this temperature was around 8 to 18^{o}C in July 2005 and 12 to 22^{o}C in September 2005. The average humidity in the laboratory during those months was between 40% and 60%.

The test cylinders were removed from the moulds one day after casting and left in laboratory ambient conditions until the day of test.

The test results plotted in Figure 4.3 show that the 7th day compressive strength of ambient-cured geopolymer concrete and the subsequent strength gain with respect to age depend on the ambient temperature at the time of casting. The 7th day compressive strength of fly ash-based geopolymer concrete increased as the average ambient temperature at casting increased. Also, the compressive strength of ambient-cured geopolymer concrete significantly increased with the age.

In contrast, as reported in Section 4.2.1 and Section 4.2.2, fly ash-based geopolymer concrete specimens cured at 60^{o} C for 24 hours reached substantially larger 7th day compressive strength than those cured in ambient conditions. Furthermore, the strength gain with age of heat-cured geopolymer concrete specimens is not significant (Figure 4.2).

The reasons for the differences in the behaviour of heat-cured versus ambient-cured fly ash-based geopolymer concrete are not clear. Fundamental research in this area is needed.

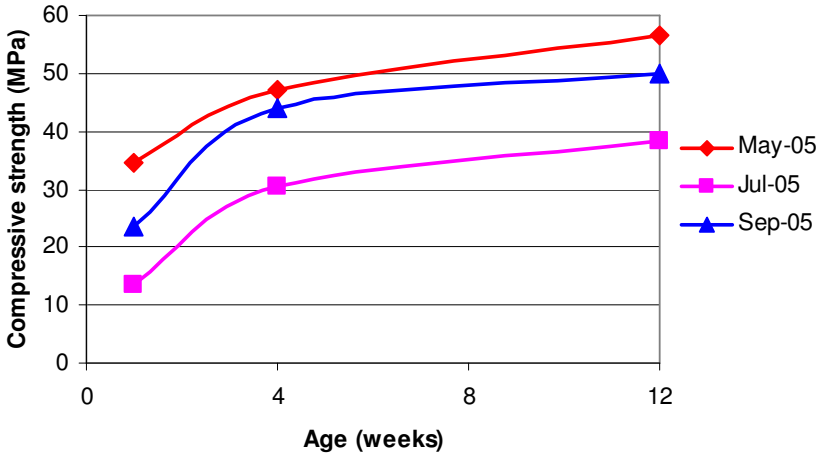

Figure 4.3 Compressive Strength of Geopolymer Concrete Cured in Ambient Condition

4.3. Creep

The creep behaviour of fly ash-based geopolymer concrete was studied for Mixture-1 and Mixture-2. The details of these Mixtures are given in Table 3.3 of Chapter 3. The test specimens were 150x300 mm cylinders. They were cured at 60^{o} C for 24 hours either by using dry curing in an oven or steam curing. The creep tests commenced on the 7th day after casting the test specimens and the sustained stress was 40% of the compressive strength on that day. The specimens made from Mixture-1 were designated as 1CR and 2CR, and those made using Mixture-2 were called 3CR and 4CR. Specimens 1CR and 3CR were dry-cured, and specimens 2CR and 4CR were steam-cured.

4.3.1. Test Results

Table 4.2 presents the 7th day compressive strength and the applied sustained stress of creep specimens. It must be noted that dry curing resulted in higher compressive strength than steam curing in the case of both Mixture-1 and Mixture-2.

Table 4.2. Compressive Strength and Sustained Stress of Creep Specimens

Test Designation	7^{th} Day compressive strength (MPa)	Sustained stress (MPa)
1CR(dry)	67	27
2CR(steam)	57	23
3CR(dry)	47	19
4CR(steam)	40	16

Table 4.3 gives the sustained stress and the instantaneous strain measured immediately after the application of the sustained load. Using these data, the instantaneous elastic modulus was calculated as sustained stress/instantaneous strain. The values of instantaneous elastic modulus, given in Table 4.3, are similar to those reported earlier for fly ash-based geopolymer concrete (Hardjito et al 2004c, Hardjito and Rangan 2005).

Table 4.3. Instantaneous Strain and Instantaneous Elastic Modulus

Test Designation	Sustained stress (MPa)	Instantaneous strain (microstrain)	Instantaneous Elastic Modulus (MPa)
1CR	27	902	29574
2CR	23	851	26852
3CR	19	828	22913
4CR	16	761	21144

Figures 4.4, 4.5, 4.6 and 4.7 present the total strain and the drying shrinkage strain measured for a period of 52 weeks (one year). The total strain was measured on the specimens in the creep test rig, while the drying shrinkage strain was obtained from the companion unloaded specimens left in the vicinity of the creep specimens.

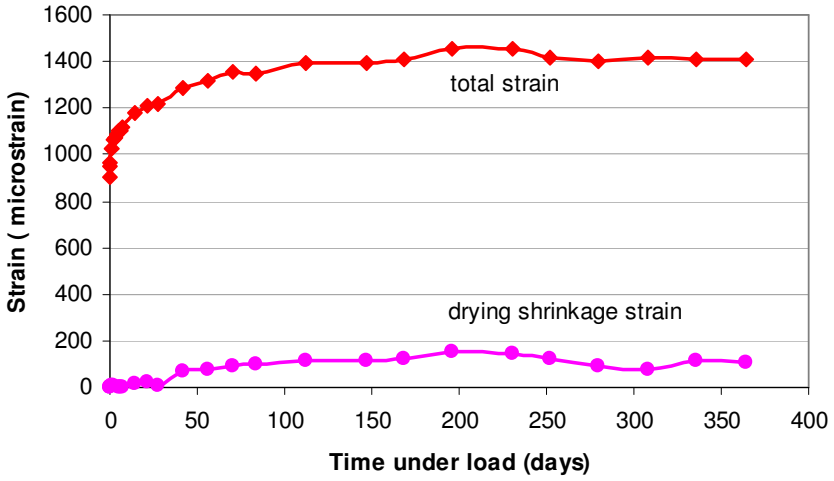

Figure 4.4 Total Strain and Drying Shrinkage Strain for 1CR

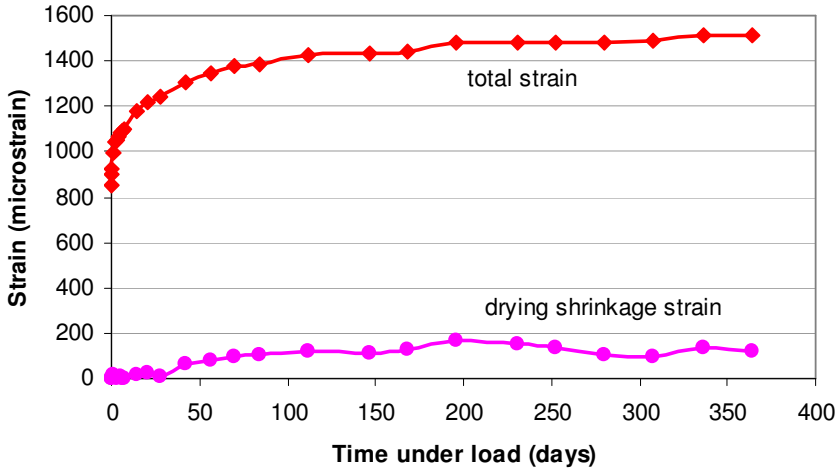

Figure 4.5 Total Strain and Drying Shrinkage Strain for 2CR

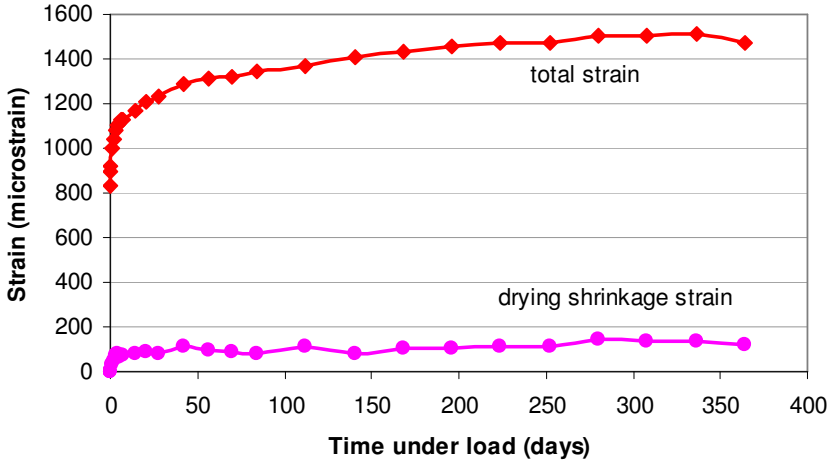

Figure 4.6 Total Strain and Drying Shrinkage Strain for 3CR

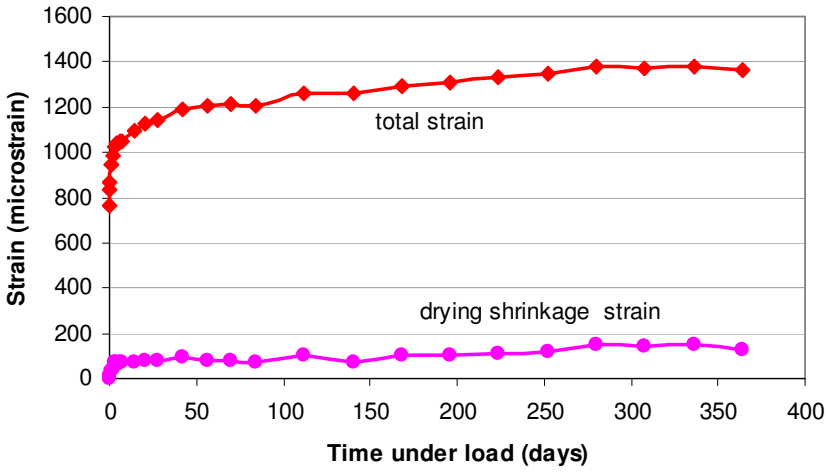

Figure 4.7 Total Strain and Drying Shrinkage Strain for 4CR

Creep strain data was obtained by subtracting the drying shrinkage strain from the total strain. The creep strain including the instantaneous elastic strain data for specimens 1CR, 2CR, 3CR, and 4CR are presented in Figures 4.8, 4.9, 4.10 and 4.11.

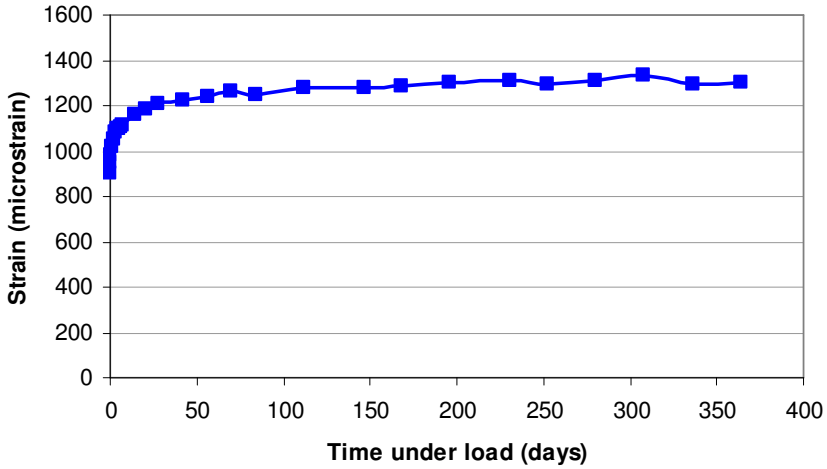

Figure 4.8 Creep Strain Data for 1CR

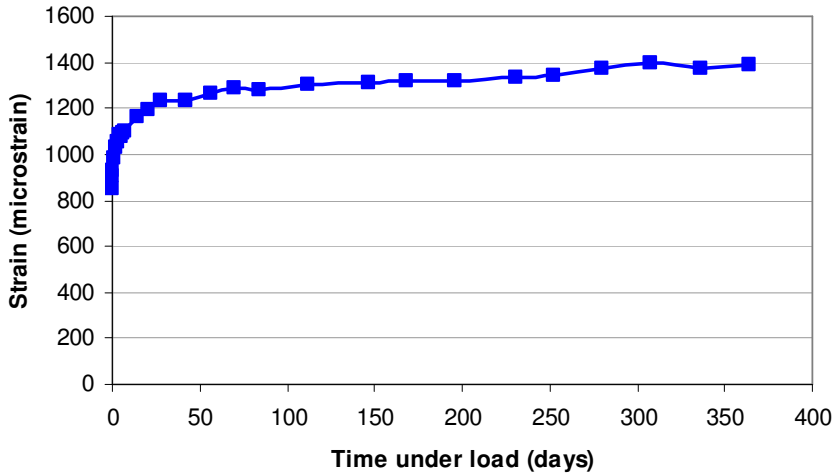

Figure 4.9 Creep Strain Data for 2CR

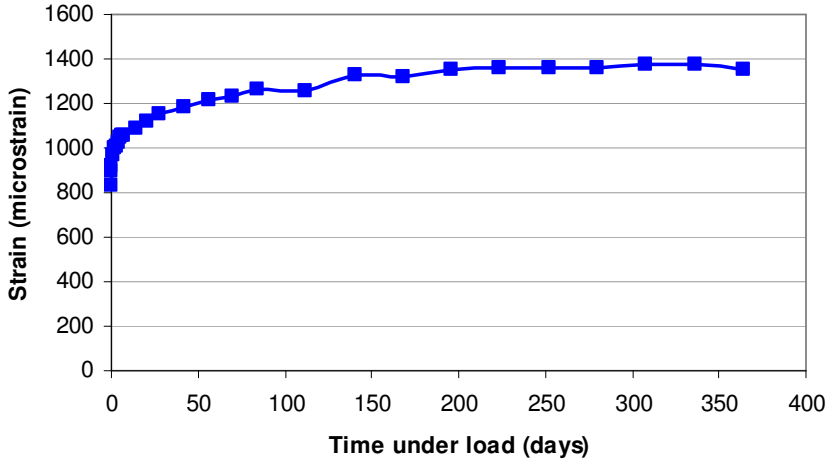

Figure 4.10 Creep Strain Data for 3CR

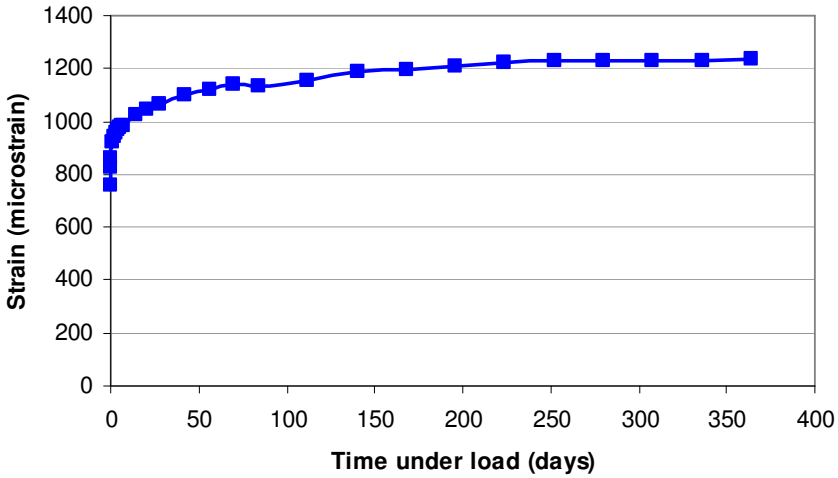

Figure 4.11 Creep Strain Data for 4CR

The creep coefficient, taken as the ratio of the creep strain to the instantaneous strain, for the test specimens are show in Figures 4.12 to 4.15.

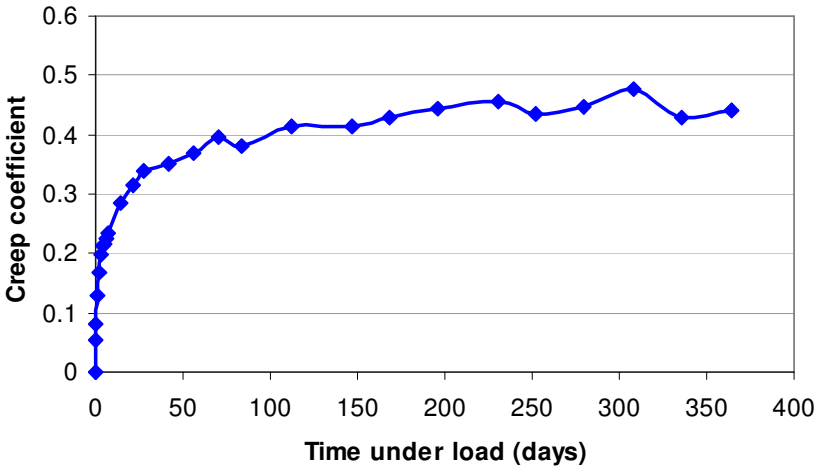

Figure 4.12 Creep Coefficient for 1CR

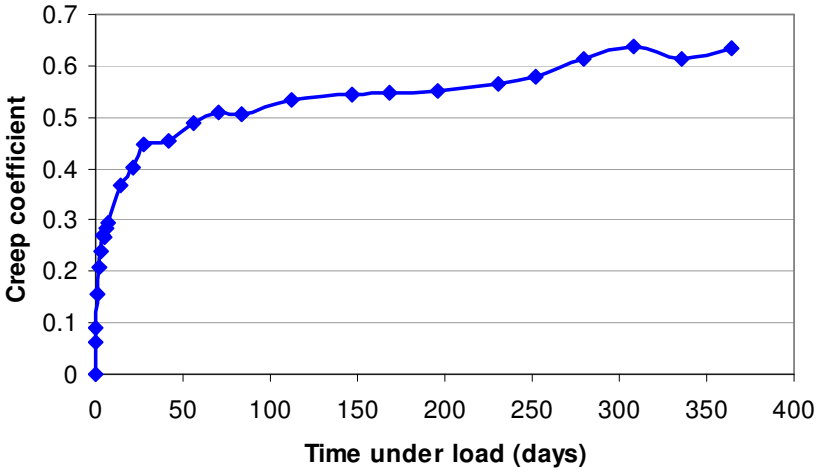

Figure 4.13 Creep Coefficient for 2CR

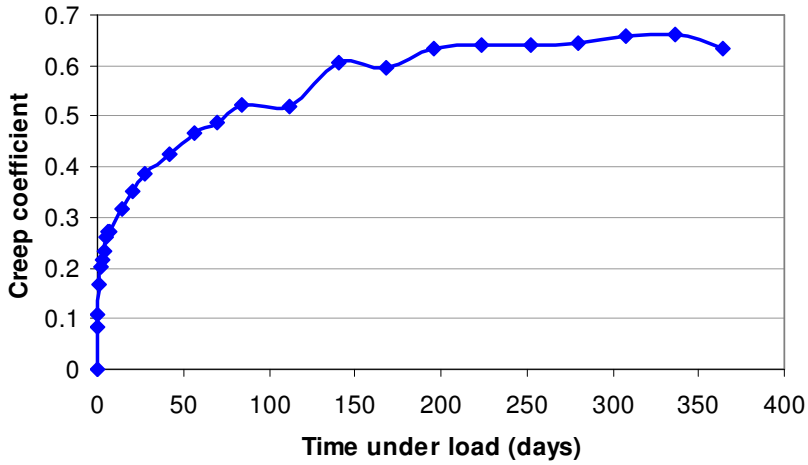

Figure 4.14 Creep Coefficient for 3CR

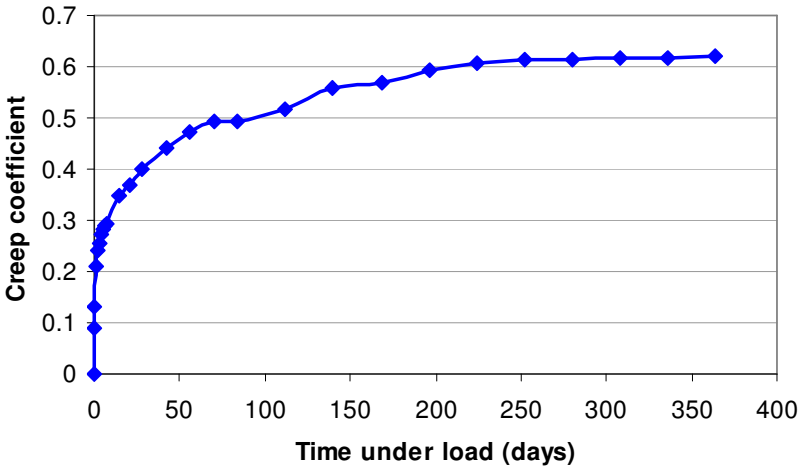

Figure 4.15 Creep Coefficient for 4CR

The specific creep, defined as the creep strain per unit stress, data for the test specimens are presented in Figure 4.16, 4.17, 4.18 and 4.19.

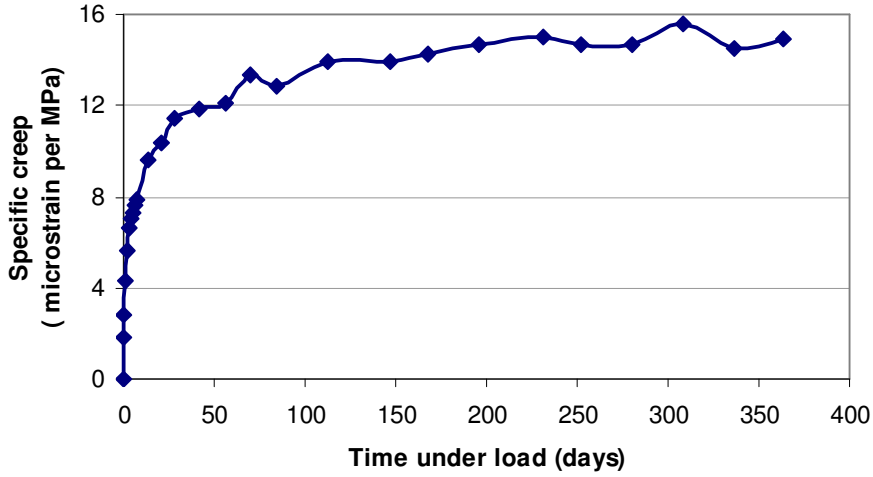

Figure 4.16 Specific Creep for 1CR

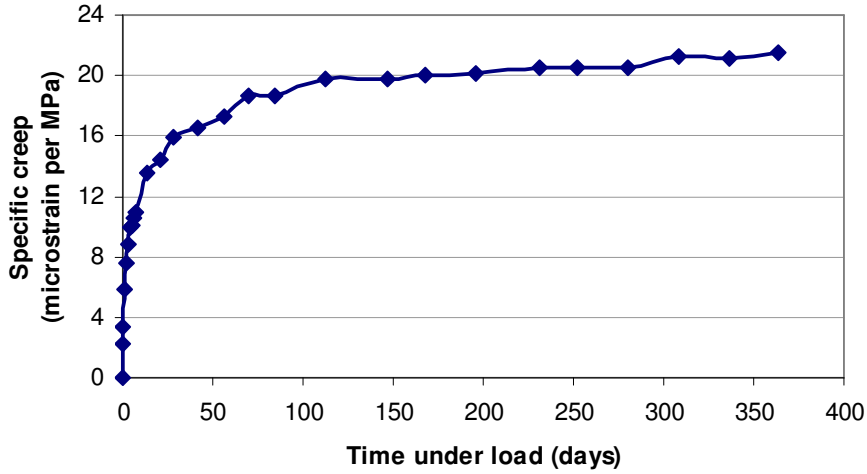

Figure 4.17 Specific Creep for 2CR

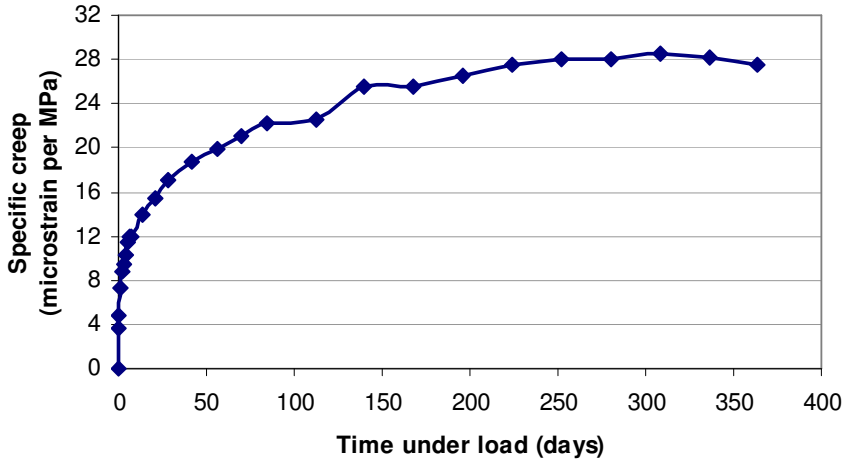

Figure 4.18 Specific Creep for 3CR

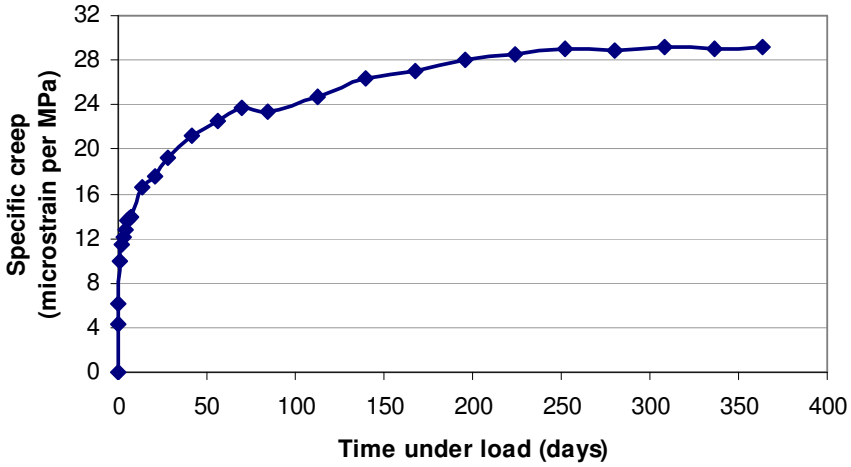

Figure 4.19 Specific Creep for 4CR

The test results in Figures 4.8 to 4.19 shows that the creep data fluctuated slightly over the period of sustained loading. This might be due to the variations in the relative humidity of the laboratory room where the creep test rig was housed.

The test results generally indicate that fly ash-based geopolymer undergoes lesser creep compared to Portland cement concrete. Warner et al (1998) illustrated that for Portland cement concrete the specific creep of 60 MPa concrete after one year was about 50 to 60 microstrain/MPa, while this value after six months was about 30 to 40 microstrain/MPa for 80 MPa concrete and about 20 to 30 microstrain/MPa for 90 MPa concrete. Similarly, Malhotra and Mehta (2002) reported that the specific creep of high-performance high volume fly ash (HVFA) concrete was about 24 to 32 microstrain/MPa after one year. Those values are generally larger than the values given in Figures 4.16 to Figure 4.19 for geopolymer concrete. This fact becomes more obvious when the creep data of geopolymer concrete are compared with the values predicted by the draft Australian Standard for Concrete Structures AS3600 (2005) as discussed in Section 4.3.3.

4.3.2. Effect of Compressive Strength

The effect of concrete compressive strength on the creep of fly ash-based geopolymer concrete is illustrated in Figure 4.20. The test data show that the specific creep of geopolymer concrete decreased as the compressive strength increased. This

test trend is similar to that observed in the case of Portland cement concrete as reported by Neville et al (1983), (Gilbert, 1988), Warner et al (1998) and Neville (2000).

The values of specific creep of geopolymer concrete after one year of loading are summarised in Table 4.4. It can be seen that the specific creep values differ significantly between geopolymer concretes with compressive strength of 47, 57, and 67 MPa, whereas this value for geopolymer concrete with compressive strength of 40 MPa is almost the same as that of 47 MPa concrete.

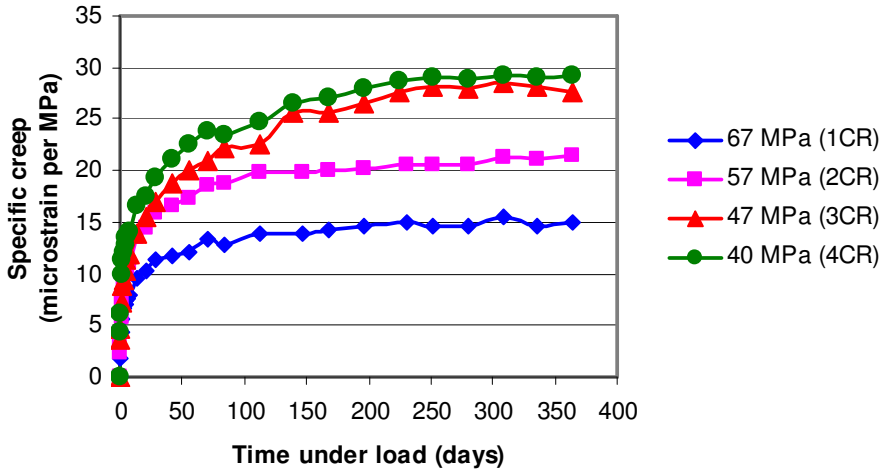

Figure 4.20 Effect of Compressive Strength on Creep of Geopolymer Concrete

Table 4.4. Specific Creep of Geopolymer Concrete

Designation	Compressive strength (MPa)	Specific creep after one year loading (x10^{-6}/MPa)
1CR	67	15
2CR	57	22
3CR	47	28
4CR	40	29

4.3.3 Correlation of Test Results with Predictions by Australian Standard AS3600

There are many methods available in the literature to predict the creep of Portland cement concrete. Based on extensive studies, Gilbert (2002) has proposed a simple

method to calculate the creep coefficient of Portland cement concrete. This method is incorporated in the draft version of the forthcoming Australian Standard for Concrete Structures AS3600 (2005). In this Section, Gilbert's method is used to predict the creep coefficients of fly ash-based geopolymer concrete reported in this work.

The Gilbert expression for calculating the creep coefficient is given by the following equation:

$$\varphi_{cc} = k_2 k_3 k_4 k_5 \varphi_{cc.b} \tag{4-1}$$

The factor k_2 , given by Equation 4-2, describes the development of creep with time and depends on the hypothetical thickness (t_h). In Equation 4-2, *t* is the time (in days) since first loading and α_2 is given by Equation 4-3.

$$k_2 = \frac{\alpha_2 t^{0.8}}{t^{0.8} + 0.15 t_h} \tag{4-2}$$

$$\alpha_2 = 1.0 + 1.12 e^{-0.008 t_h} \tag{4-3}$$

The factor k_3 is the maturity coefficient as given by Figure 4.21. For the strength ratio, f'_c is the characteristic compressive cylinder strength of concrete at 28 days and f_{cm} is the mean value of the compressive strength of concrete at relevant age.

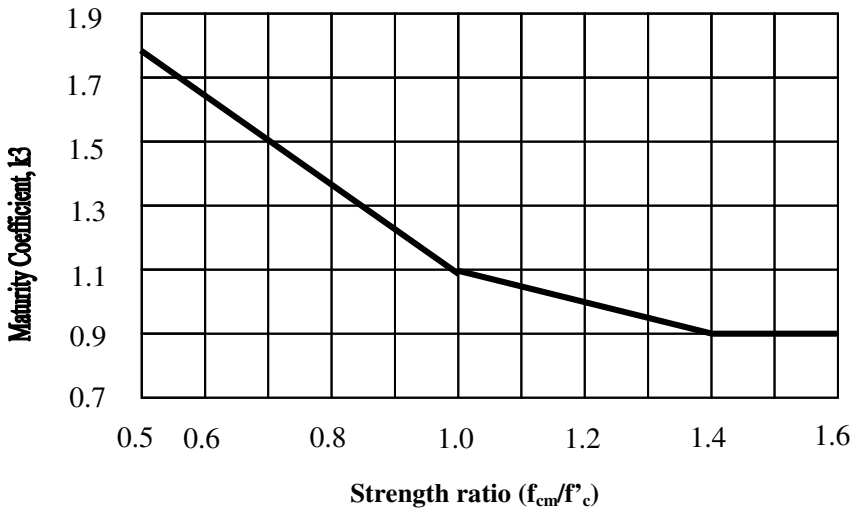

Figure 4.21 Maturity Coefficient k_3 (Gilbert 2002)

The factor k_4 accounts for the environment and is taken equal to 0.7 for an arid environment, 0.65 for an interior environment, 0.60 for a temperate environment and 0.5 for a tropical/coastal environment.

The factor k_5 accounts for the relative humidity and the member size and is given by Equations 4-4a and 4-4b.

When $f'_c \leq 50$ MPa:

$$k_5 = 1.0 \qquad (4\text{-}4a)$$

When 50 MPa $< f'_c \leq 100$ MPa:

$$k_5 = (2.0 - \alpha_3) - 0.02\,(1.0 - \alpha_3)\, f'_c \qquad (4\text{-}4b)$$

Where

$$\alpha_3 = \frac{0.7}{k_4 \alpha_2} \qquad (4\text{-}5)$$

The hypothetical thickness (t_h) is given by Equation 4-6, where A is the cross-sectional area of the member and u_e is that part of the perimeter of the member cross-section which is exposed to the atmosphere.

$$t_h = \frac{2A}{u_e} \qquad (4\text{-}6)$$

The basic creep coefficient ($\varphi_{cc.b}$) is given in Table 4.5.

Table 4.5 Basic Creep Coefficient (Gilbert 2002)

f'_c (MPa)	20	25	32	40	50	65	80	100
$\varphi_{cc.b}$	5.2	4.2	3.4	2.8	2.4	2.0	1.7	1.5

The comparison of the experimental results with the values calculated by Gilbert's method is given in Figures 4.22 to 4.25. The details of the calculations are given in Appendix A. Because the effect of age on the compressive strength of heat-cured fly ash-based geopolymer concrete is not significant (see Section 4.2.2), the strength ratio f_{cm}/f'_c is taken as equal to 1.0 and the maturity coefficient, $k_3 = 1.1$ (Figure

4.21). The environmental factor, k_4 is taken as equal to 0.65 (interior environment) because the creep tests were conducted in an interior environment.

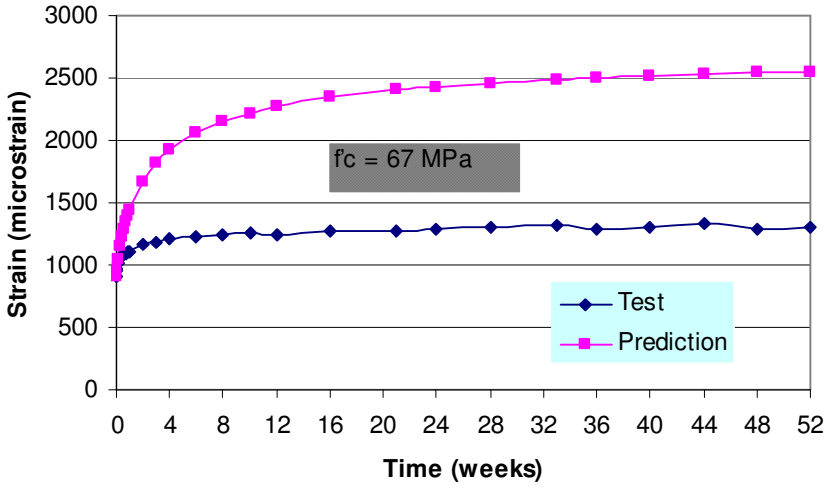

Figure 4.22 Correlation of Test and Predicted Creep Strain Data: Specimen 1CR

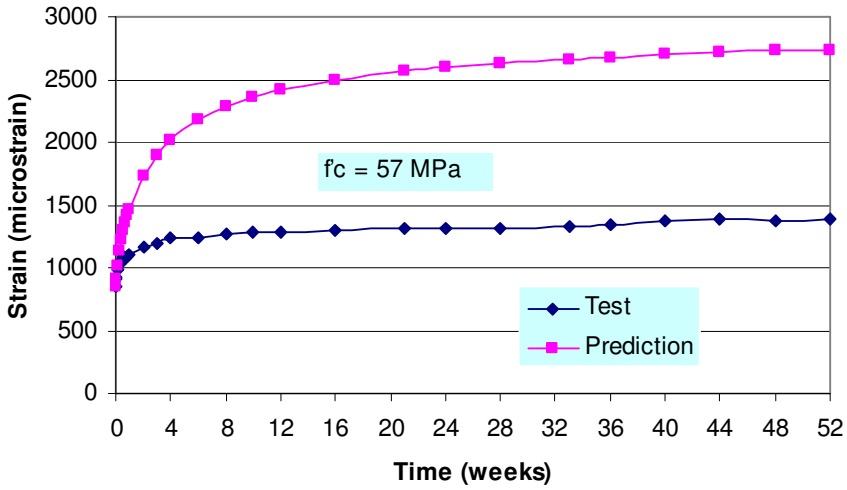

Figure 4.23 Correlation of Test and Predicted Creep Strain Data: Specimen 2CR

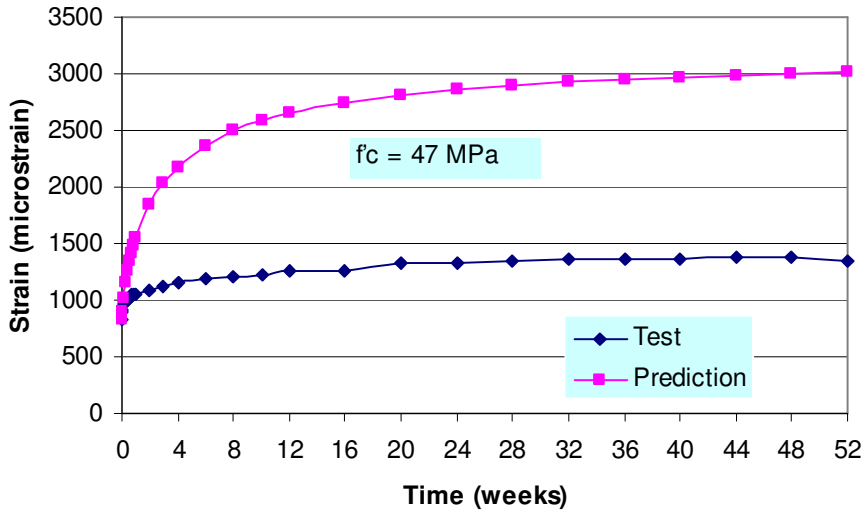

Figure 4.24 Correlation of Test and Predicted Creep Strain Data: Specimen 3CR

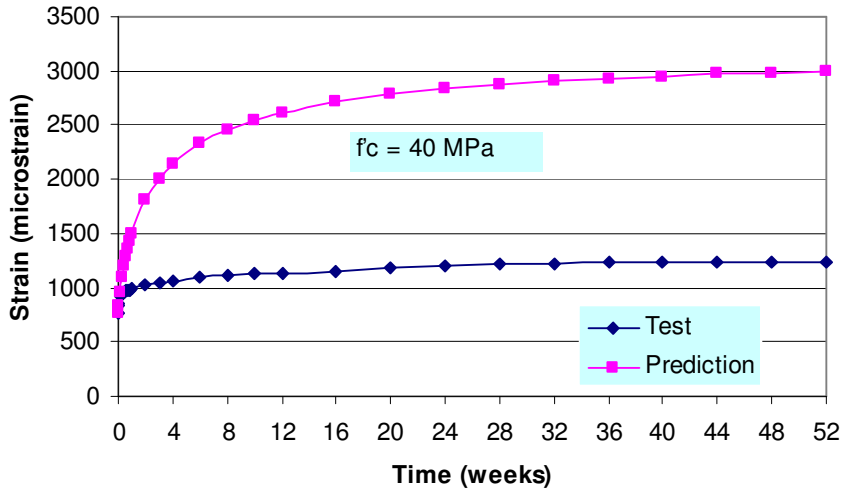

Figure 4.25 Correlation of Test and Predicted Creep Strain Data: Specimen 4CR

Figures 4.22 to 4.25 show that the measured strains of fly ash-based geopolymer concrete are significantly smaller than the predicted values. As discussed earlier in Section 4.3.1, the creep strains of fly ash-based geopolymer concrete are generally smaller than that of Portland cement concrete. The exact reasons for this difference in behaviour are not known. However, it has been suggested by Davidovits (2005a) that the smaller creep strains of fly ash-based geopolymer concrete may be due to 'block-polymerisation' concept. According to this concept, the silicon and aluminium atoms in the fly ash are not entirely dissolved by the alkaline liquid. The

'polymerisation' that takes place only on the surface of the atoms is sufficient to form the 'blocks' necessary to produce the geopolymer binder. Therefore, the insides of the atoms are not destroyed and remain stable, so that they can act as 'micro-aggregates' in the system.

In Portland cement concrete, the creep is primarily caused by the cement paste. The aggregates are generally inert component of the mixtures, and function to resist the creep of the cement paste. Therefore, the aggregate content in the concrete is a significant factor influencing the creep of the concrete as the creep will decrease with the increase in the quantity of the aggregates. The proportion of aggregates in the mixtures of fly ash-based geopolymer concrete used in this work is approximately similar to that used in Portland cement concrete. However, the presence of the 'micro-aggregates' due to the 'block-polymerisation' concept mentioned above gives the effect of increasing the aggregate content in the concrete. In other words, the presence of the 'micro-aggregates' increases the creep resisting function of the fly ash-based geopolymer concrete which results in smaller creep compared to Portland cement concrete without 'micro-aggregates'.

4.4. Drying Shrinkage

The drying shrinkage behaviour of fly ash-based geopolymer concrete was studied for Mixture-1 and Mixture-2. The proportions of these Mixtures and the details of the drying shrinkage tests are given in Chapter 3. The drying shrinkage measurements commenced on the third day after casting. Therefore, the age 'zero' in the drying shrinkage strain versus age in days plots shown in Figures 4.26 to 4.33 represents three days after casting when the first initial measurements were taken.

4.4.1. Drying Shrinkage of Heat-cured Geopolymer Concrete Specimens

The test specimens, heat-cured at 60^{o}C for 24 hours, were identified as given in Table 4.6. The 7^{th} day compressive strengths of the Mixtures are also given in Table 4.6.

Table 4.6. Heat-cured Geopolymer Concrete Shrinkage Specimens

Test Designation	Type of mixture	Curing type	7^{th} Day compressive strength (MPa)
1DS	Mixture-1	dry	65
2DS	Mixture-1	steam	57
3DS	Mixture-2	dry	50
4DS	Mixture-2	steam	41

Figures 4.26 and 4.27 show the drying shrinkage strain versus age in days plots of heat-cured test specimens. It can be seen from these Figures that heat-cured fly ash-based geopolymer concrete undergoes very low drying shrinkage. For all test specimens, the drying shrinkage strain after one-year period was only around 100 micro strains.

The test data plotted in Figures 4.26 and 4.27 show that the drying shrinkage strains fluctuated slightly over the period of measurement. This could be attributed to the moisture movement from the environment to the concrete or vice versa which causes reversible shrinkage or swelling of the concrete. Also, there were some minor differences in the measured values of drying shrinkage strains between dry and steam cured specimens. However, these variations are considered to be insignificant in the context of the very low drying shrinkage experienced by the heat-cured geopolymer concrete specimens.

Water is released during the chemical reaction process of geopolymers (Davidovits 1999, Hardjito and Rangan 2005). In heat-cured fly ash-based geopolymer concrete, most of the water released during the chemical reaction may evaporate during the curing process. Because the remaining water contained in the micro-pores of the hardened concrete is small, the induced drying shrinkage is also very low. In addition, as for the creep (see Section 4.3.3), the presence of the 'micro-aggregates' in fly ash-based geopolymer concrete may also increase the restraining effect of the aggregates on drying shrinkage.

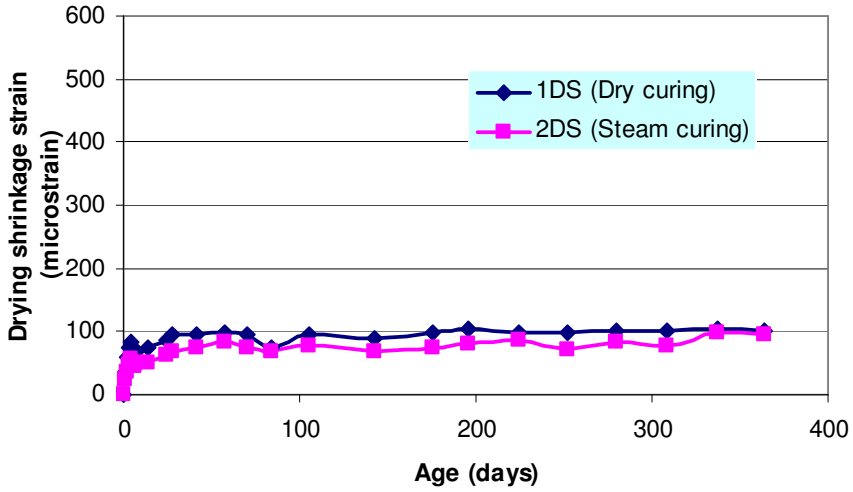

Figure 4.26 Drying Shrinkage of Heat-cured Mixture-1 Specimens

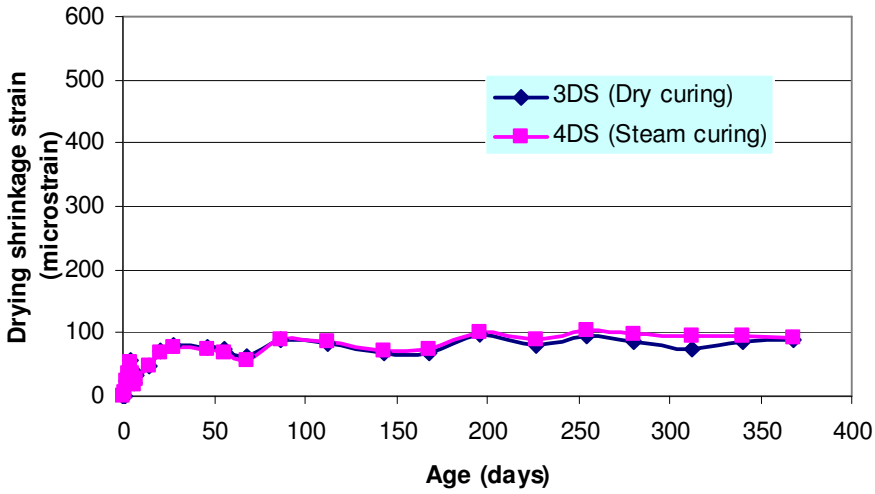

Figure 4.27 Drying Shrinkage of Heat-cured Mixture-2 Specimens

4.4.2. Drying Shrinkage of Heat-cured Specimens versus Ambient-cured Specimens

A series of drying shrinkage specimens, designated as 5DS, were made using a batch of Mixture-1. One set of these specimens was left in the ambient conditions of the laboratory and another set of specimens was heat-cured in the oven at 60^{o}C for 24 hours. These sets of specimens were cast in November 2005. The test results obtained from these two sets of specimens are presented in Figure 4.28. The 7th day compressive strength of the specimens was 27 MPa for ambient-cured specimens and 61 MPa for heat-cured specimens.

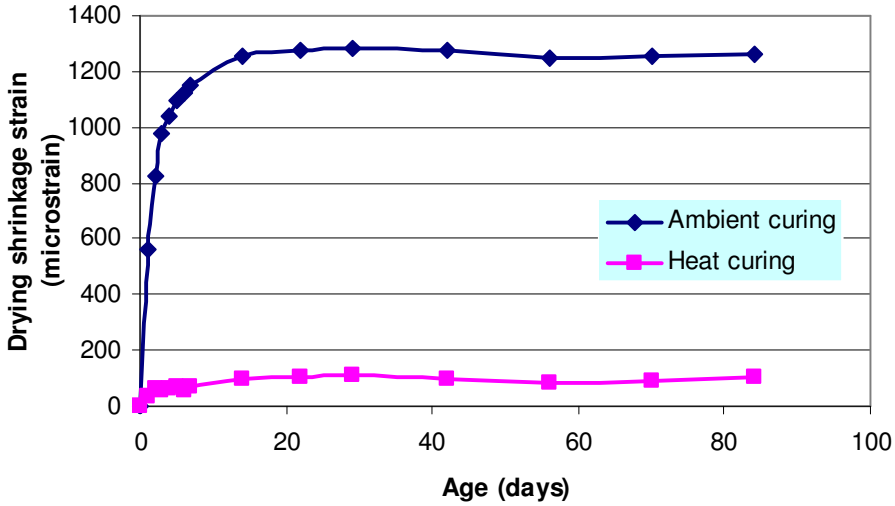

Figure 4.28 Drying Shrinkage of Heat-cured and Ambient-cured Specimens

It can be seen that the drying shrinkage strains of the specimens cured in ambient conditions are many folds larger than those experienced by the heat-cured specimens. As noted earlier, water is released during chemical reaction process of geopolymers. In the specimens cured in ambient conditions, this water may evaporate over a period of time causing significantly large drying shrinkage strains especially in first two weeks as can be seen in Figure 4.28.

4.4.3 Correlation of Test results with Predictions by Australian Standard AS3600

The measured drying shrinkage strains are compared with the values predicted by a method proposed by Gilbert (2002) for inclusion in the forthcoming Australian Standard for Concrete Structures AS3600 (2005).

The method proposed by Gilbert divides the total shrinkage strain (ε_{cs}) into endogenous shrinkage (ε_{cse}) and drying shrinkage (ε_{csd}). Endogenous shrinkage is taken as the sum of chemical shrinkage and thermal shrinkage. The total shrinkage strain is given by Equation 4-7 and the endogenous shrinkage at any time t (in days) after concrete placement is given by Equation 4-8.

$$\varepsilon_{cs} = \varepsilon_{cse} + \varepsilon_{csd} \qquad (4\text{-}7)$$

$$\varepsilon_{cse} = \varepsilon_{cse} * (1.0 - e^{-0.1t}) \quad (4\text{-}8)$$

Where ε_{cse}^* is the final endogenous shrinkage and may be taken as

$$\varepsilon_{cse}^{*} = (0.06\ f'_c - 1.0) \times 50 \times 10^{-6} \quad (4\text{-}9)$$

in which f'_c is in MPa.

The drying shrinkage at time t (in days) after the commencement of drying may be taken as

$$\varepsilon_{csd} = k_1 k_4 \varepsilon_{csd.b} \quad (4\text{-}10)$$

where $\varepsilon_{csd.b}$ is given by Equation 4-11. In Equation 4-11, $\varepsilon_{csd.b}^*$ depends on the quality of the local aggregates and may be taken as 800 x 10^{-6} for Sydney and Brisbane, 900 x 10^{-6} for Melbourne and 1000 x 10^{-6} elsewhere.

$$\varepsilon_{csd.b} = (1.0 - 0.008 f'_c) \times \varepsilon_{csd.b}^{*} \quad (4\text{-}11)$$

The factor k_1 in Equation 4-10 is given by Equation 4-12, and the factor k_4, as for creep as discussed previously, is taken equal to 0.7 for an arid environment, 0.65 for an interior environment, 0.6 for a temperate inland environment and 0.5 for a tropical or near-coastal environment.

$$k_1 = \frac{\alpha_1 t^{0.8}}{t^{0.8} + 0.15 t_h} \quad (4\text{-}12)$$

where

$$\alpha_1 = 0.8 + 1.2 e^{-0.005 t_h} \quad (4\text{-}13)$$

and the hypothetical thickness, t_h is the same as is given by Equation 4-6.

The measured shrinkage strains are compared with the predictions by Gilbert method in Figures 4.29 to 4.33. In these calculations, the factor k_4 was taken as equal to 0.65 as the test specimens were exposed to an interior environment and the value of f'_c

was taken as the 7th day compressive strength of the test specimens as given in Table 4.6 and in Section 4.4.2.

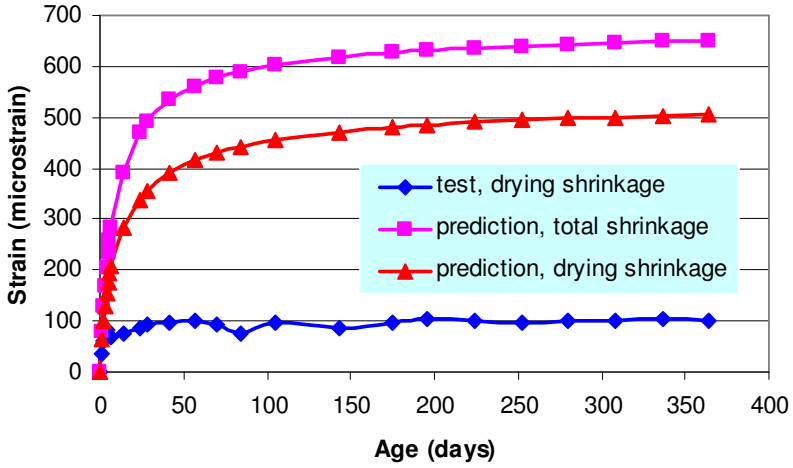

Figure 4.29 Comparison of Test and Predicted Shrinkage Strains for 1DS

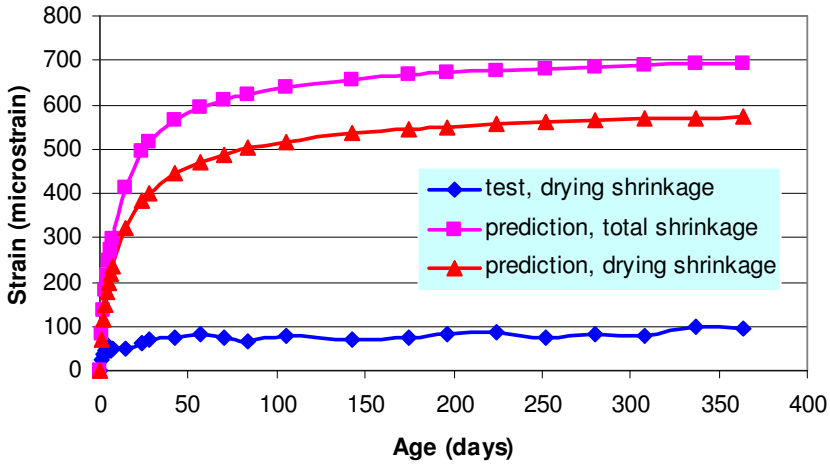

Figure 4.30 Comparison of Test and Predicted Shrinkage Strains for 2DS

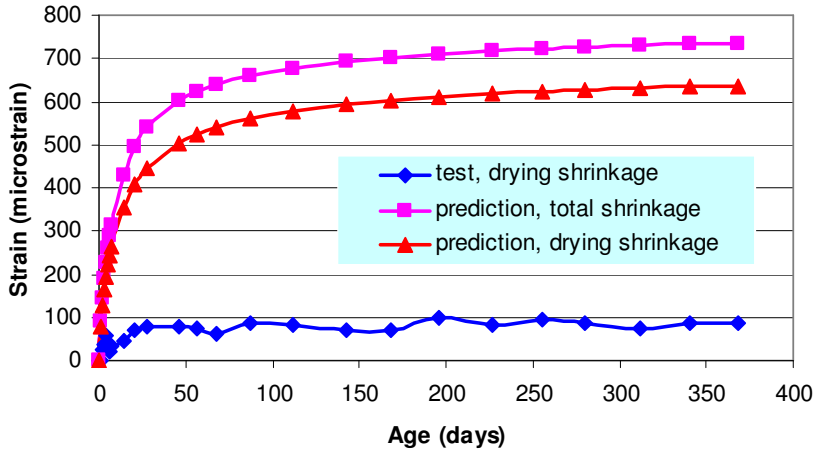

Figure 4.31 Comparison of Test and Predicted Shrinkage Strains for 3DS

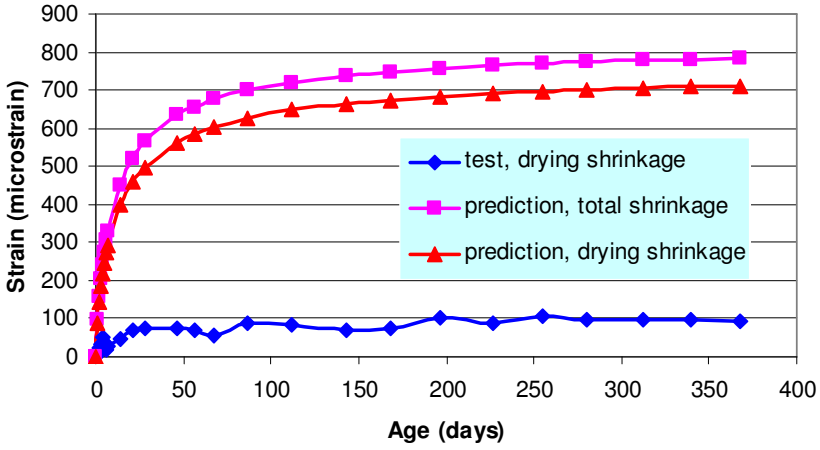

Figure 4.32 Comparison of Test and Predicted Shrinkage Strains for 4DS

It can be seen from Figures 4.29 to 4.32 that the measured drying shrinkage strains of heat-cured fly ash-based geopolymer concrete specimens are significantly smaller than the predicted values. On the other hand, for the specimens cured in ambient conditions (Figure 4.33), the drying shrinkage strains are significantly larger than the predicted values.

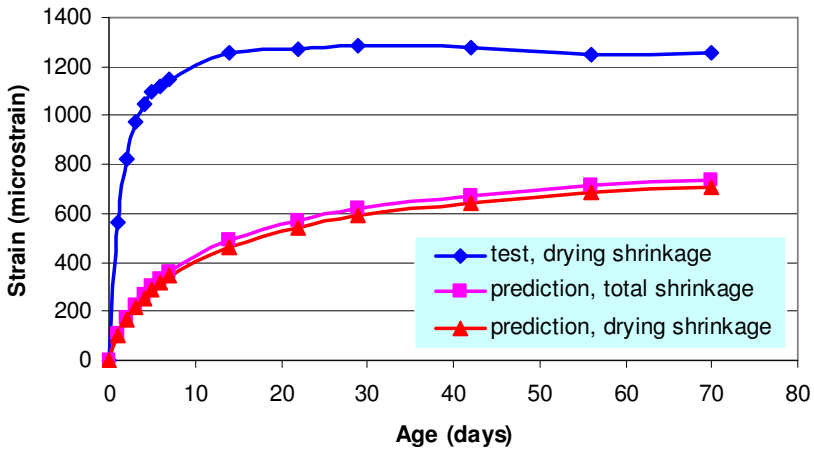

Figure 4.33 Comparison of Test and Predicted Shrinkage Strains for 5DS

4.5. Sulfate Resistance

A series of tests were performed to study the sulfate resistance of fly ash-based geopolymer concrete. The details of the tests are described in Chapter 3. The test specimens were soaked in 5% sodium sulfate (Na_2SO_4) solution. The sulfate resistance was evaluated based on visual appearance, change in length, change in mass, and change in compressive strength after sulfate exposure up to one year period. All specimens were made using Mixture-1. The change in mass and change in length test specimens were made using fly ash from Batch-1, while fly ash from Batch-2 was used for the change in compressive strength test specimens. For comparison, some specimens were soaked in tap water and some were left in the laboratory ambient conditions. All specimens were heat-cured at 60^{o}C for 24 hours.

4.5.1. Visual Appearance

The visual appearances of test specimens after different exposures are shown in Figure 4.34. It can be seen that the visual appearance of the test specimens after soaking in sodium sulfate solution up to one year revealed that there was no change in the appearance of the specimens compared to the condition before they were exposed. There was no sign of surface erosion, cracking or spalling on the

specimens. The specimens soaked in tap water also showed no change in the visual appearance (Figure 4.34).

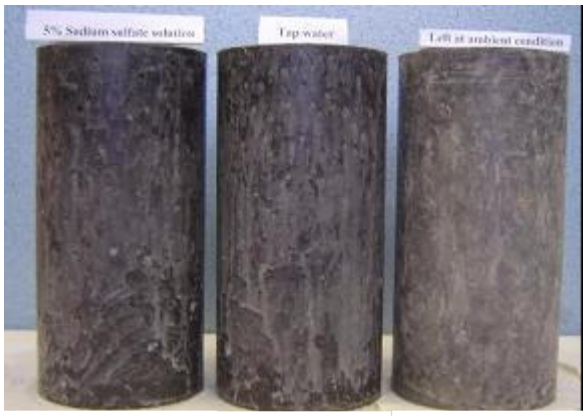

Figure 4.34 Visual Appearance of Geopolymer Concrete Specimens after One Year of Exposure

4.5.2. Change in Length

Test results on the change in length of the specimens soaked in sodium sulfate solution up to one year period are presented in Figure 4.35. It can be seen that the change in length is extremely small and less than 0.015%.

Tikalsky and Carasquillo (1992) stated that concrete specimens that suffer an expansion in the order of 0.5% must be considered as failed under sulphate attack. The change in length of 0.015% experienced by heat-cured geopolymer concrete is far from this limit of 0.5%. The change in length of geopolymer concrete is also smaller than that of Portland cement concrete. For example, Wee et al (2000) observed that the change in length of Portland cement concrete with water/binder ratio of 0.4 to 0.5 was about 0.035 to 0.1% after 32 weeks of immersion in 5% sodium sulfate solution.

Therefore, the test results shown in Figure 4.35 demonstrate that the heat-cured fly ash-based geopolymer concrete has excellent resistance to sulphate attack.

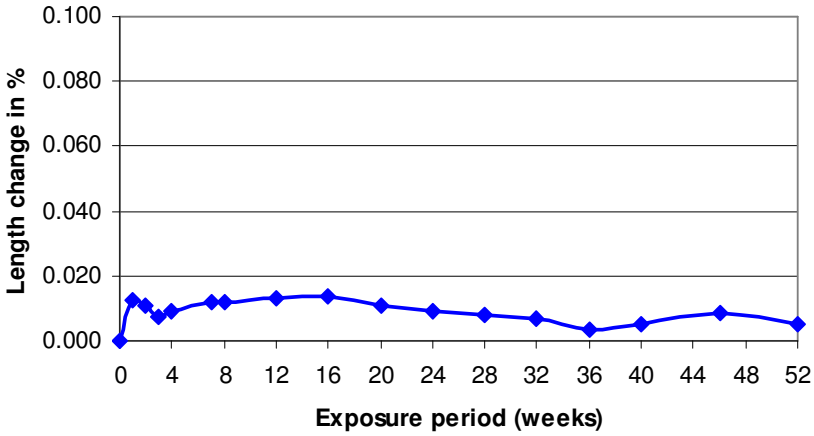

Figure 4.35 Change in Length of Geopolymer Concrete Specimens Exposed to Sodium Sulfate Solution

4.5.3. Change in Mass

Figure 4.36 presents the test results on the change in mass of specimens soaked in sodium sulfate solution up to one year period as a percentage of the mass before exposure. For comparison, Figure 4.36 also presents the change in mass of specimens soaked in water for the corresponding period. It can be seen that there was no reduction in the mass of the specimens, as confirmed by the visual appearance of the specimens in Figure 4.34. There was a slight increase in the mass of specimens due to the absorption of the exposed liquid. The increase in mass of specimens soaked in sodium sulphate solution was approximately 1.5% after one year of exposure. In the case of specimens soaked in tap water, this increase in mass was about 1.8%.

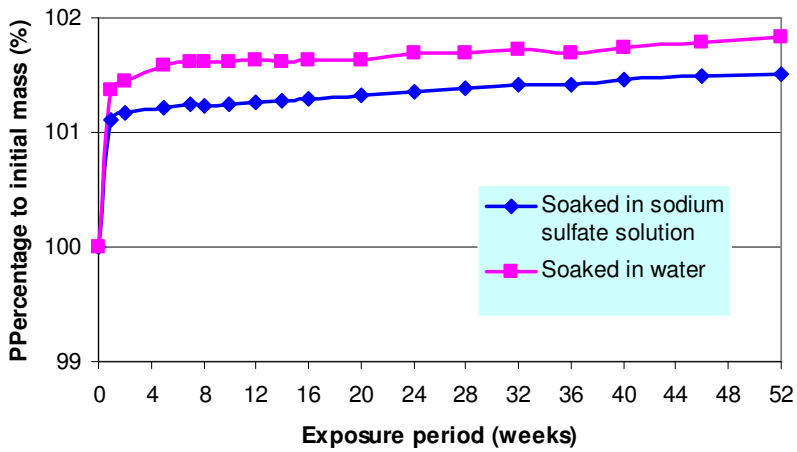

Figure 4.36 Change in Mass of Specimens Soaked in Sodium Sulfate Solution and Water

4.5.4. Change in Compressive Strength

Change in compressive strength was determined by testing the specimens after 4 weeks, 8 weeks, 12 weeks, 24 weeks and 52 weeks (1 year) of soaking in sulphate solution. For each period of exposure, the test specimens were made using a different batch of geopolymer concrete (Mixture-1). For comparison, for every period of exposure, a set of specimens from the same batch was also prepared, soaked in tap water, and tested for compressive strength. Another set of specimens from the same batch was also made and tested for compressive strength on the seventh day after casting. The compressive strength of these specimens without any exposure was taken as the reference compressive strength.

The test specimens soaked in liquids were removed from the immersion container, wiped clean, and tested immediately in saturated-surface-dry (SSD) condition. The test results for various exposure periods are presented in Figure 4.37 to Figure 4.41.

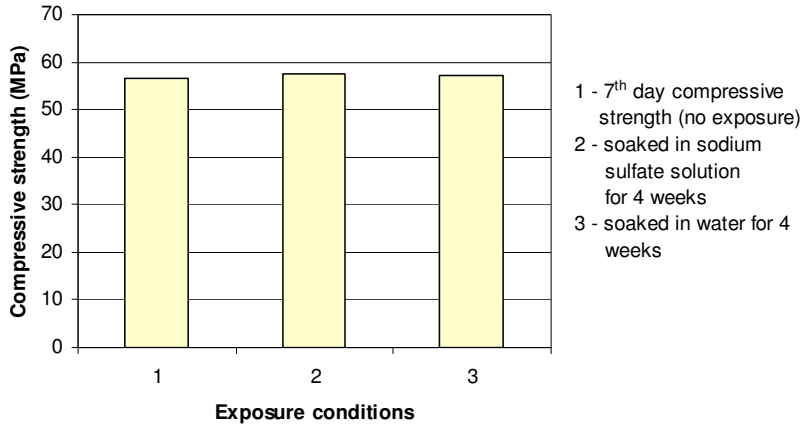

Figure 4.37 Compressive Strength of Geopolymer concrete After 4 Weeks of Exposure

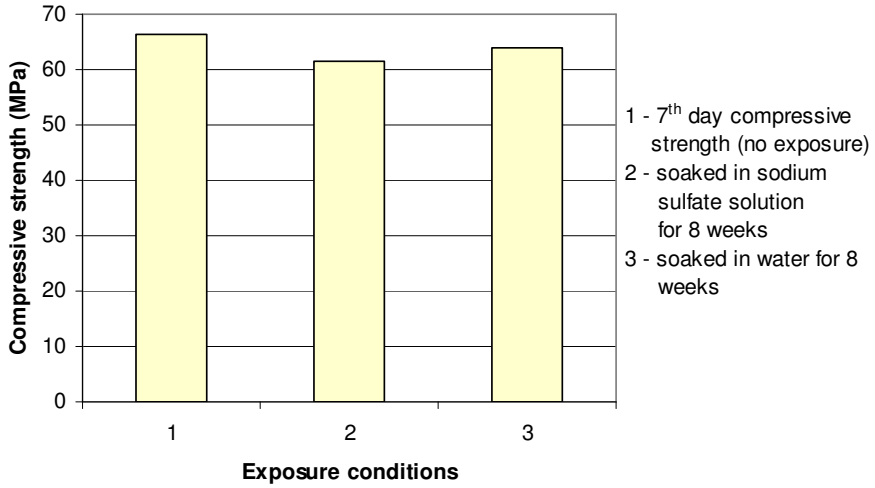

Figure 4.38 Compressive Strength of Geopolymer Concrete After 8 Weeks of Exposure

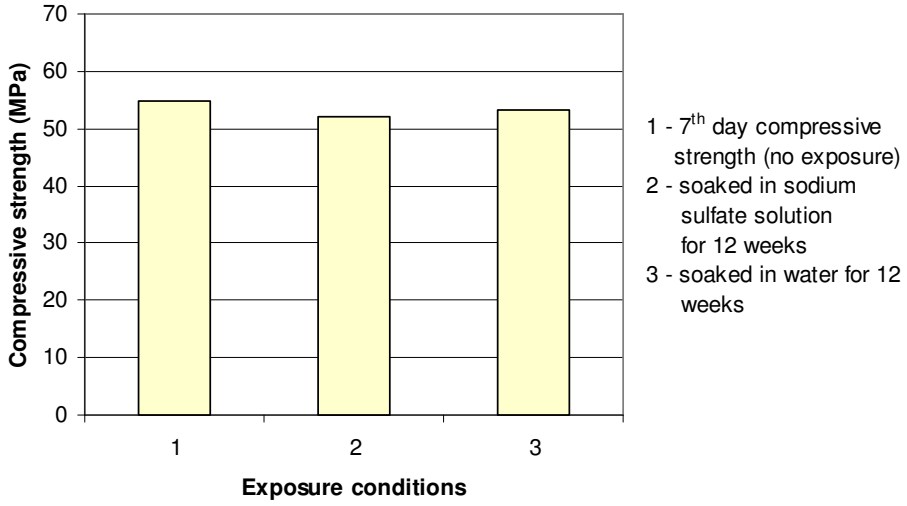

Figure 4.39 Compressive Strength of Geopolymer Concrete After 12 Weeks of Exposure

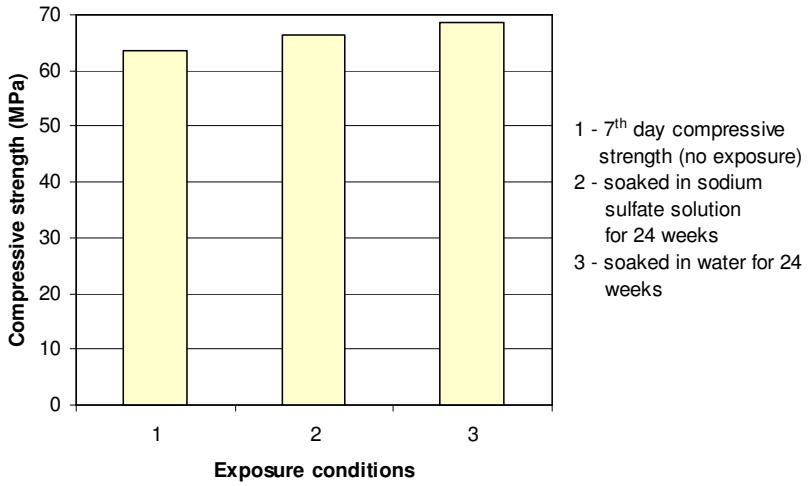

Figure 4.40 Compressive Strength of Geopolymer Concrete After 24 Weeks of Exposure

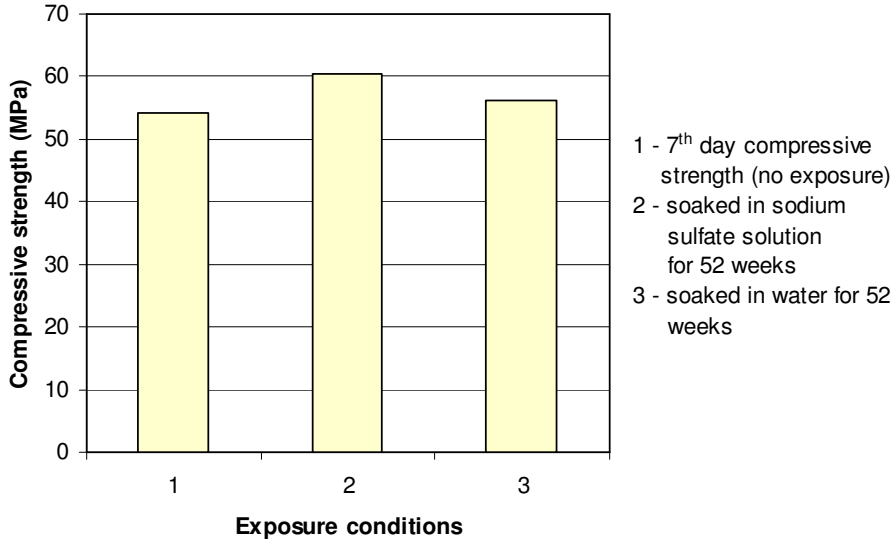

Figure 4.41 Compressive Strength of Geopolymer Concrete After 52 Weeks of Exposure

The test data shown in Figures 4.37 to 4.41 are recast in the first three columns of Table 4.7 in the form of ratio of compressive strength after periods of exposure to the reference 7th day compressive strength of specimens with no exposure. These test results show that exposure of heat-cured fly ash-based geopolymer concrete to 5% sodium sulfate solution caused very little change in the compressive strength.

In order to study the effect of specimen condition at the time of test on the compressive strength of specimens exposed to sulfate solution, another set of specimens were made using a single batch of Mixture-1. After various periods of exposure, the specimens were removed from the sulfate solution and left to dry in the laboratory ambient conditions for about one week before testing. The results of these tests are presented in Table 4.7 under the heading 'Dry condition'. The trend of these test data is also similar to that observed for the specimens tested in SSD condition.

Table 4.7 Change in Compressive Strength of Geopolymer Concrete for Different Test Conditions

Exposure period (weeks)	Ratio of compressive strength to 7th day compressive strength (no exposure), %			
	SSD condition		Dry condition	
	Sulfate exposure	Water exposure	Sulfate exposure	Water exposure
4	102	101	103	*
8	93	96	*	*
12	95	97	107	*
24	105	108	102	*
36	*	*	107	*
52	111	103	111	*

** Not tested*

It can also be seen from Table 4.7 that the period of exposure seems not to have considerable effect on the compressive strength. The variations in the data are considered to be insignificant. Test results also indicate that the effect of condition of specimens at the time of compression test (SSD or Dry condition) is insignificant. As can be seen from Table 4.7, the difference and the variation of the compressive strength for various periods of exposure for both the conditions are marginal.

The deterioration of Portland cement concrete due to sulfate attack can be attributed to the formation of expansive gypsum and ettringite which can cause expansion, cracking and spalling in the concrete. Sulfates can react with various products of hydrated cement paste to form gypsum and ettringite (Lea, 1970; Neville, 2000). Sulfate ions in concrete could react with portlandite to form gypsum or react with calcium aluminate hydrate to form calcium sulfoaluminate or ettringite. The formation of gypsum and ettringite due to sulfate attack is very expansive since these elements could absorb moisture so that their volume of solid phase could increase to about 124% and 227%. Mehta (1983) also stated that the sulfate attack could lower the stiffness of the cement paste and increase the water-absorption capacity of the ettringite. Besides the disruptive expansion and cracking, sulfate attack could also cause loss of strength of concrete due to the loss of cohesion in the hydrated cement paste and of adhesion between it and aggregate particles (Neville, 2000).

Various studies have been reported to identify the role of fly ash as supplementary cementing material in Portland cement concrete in improving the sulfate resistance concrete (Malhotra & Mehta, 2002; Tikalsky & Carrasquillo, 1992; Torii et. al., 1995). Some important factors identified which contributes to better resistance to sulfate attack include the low content of calcium oxide in fly ash or calcium hydroxide in concrete and the fine and discontinuous pore structure that results in low permeability.

Fly ash-based geopolymer concrete undergoes a different mechanism to that of Portland cement concrete and the geopolymerisation products are also different from hydration products. The main product of geopolymerisation, as given by Equation 2-2 is not susceptible to sulfate attack like the hydration products. Because there is generally no gypsum or ettringite formation in the main products of geopolymerisation, there is no mechanism of sulfate attack in fly ash-based geopolymer concrete. However, to some extent, the formation of gypsum and ettringite might happen depending on the presence of calcium in the concrete as identified by Song et al (2005b). The source of calcium could be either from the fly ash or the aggregates.

In the present work, low-calcium fly ash was used as the source material. The test results presented in this Section clearly demonstrate the excellent resistance of heat-cured low-calcium fly ash-based geopolymer concrete to sulfate attack.

4.6. Acid Resistance

Acid resistance of fly ash-based geopolymer concrete was studied by soaking concrete and mortar specimens in various concentrations of sulfuric acid solution up to one year, and by evaluating the behaviour in terms of visual appearance, change in mass and change in compressive strength after exposure. Mixture-1 (Table 3.3) was used to manufacture the concrete specimens and, the mortar specimens were made using the mixture proportion given in Table 3.4. Fly ash from Batch-2 was used for all concrete and mortar specimens. The test specimens were heat-cured at 60^{o}C for 24 hours. The sulphuric acid solution was stirred each week and was replaced every month.

4.6.1. Visual Appearance

Figure 4.42 compares the visual appearance of the geopolymer concrete specimens after soaking in various concentrations of sulfuric acid solution for a period of one year with the specimen without acid exposure and left in ambient conditions of the laboratory. It can be seen that the specimens exposed to sulfuric acid undergoes erosion of the surface. The damage to the surface of the specimens increased as the concentration of the acid solution increased.

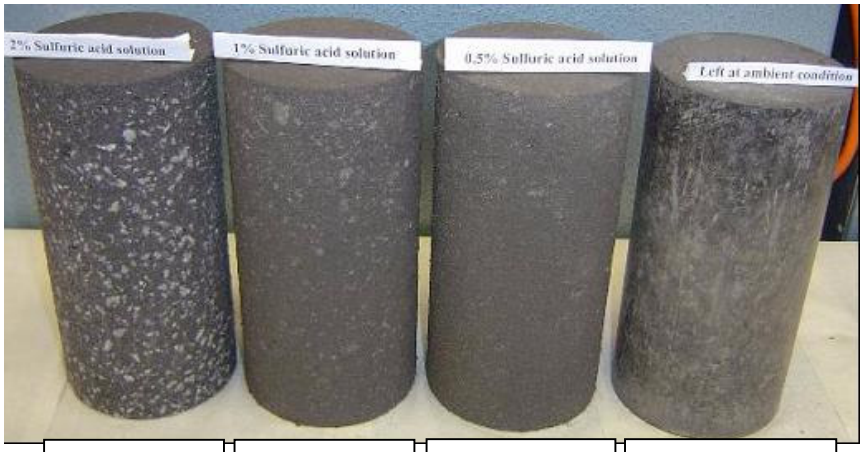

Figure 4.42 Visual Appearance after One Year Exposure in Sulfuric Acid Solution

Erosion of specimen surfaces was also observed in geopolymer mortar specimens after one year of exposure in sulfuric acid solution, as shown in Figure 4.43. The severity of the damage and the distortion of the shape of specimens depended on the concentration of the solution, as seen in Figure 4.43.

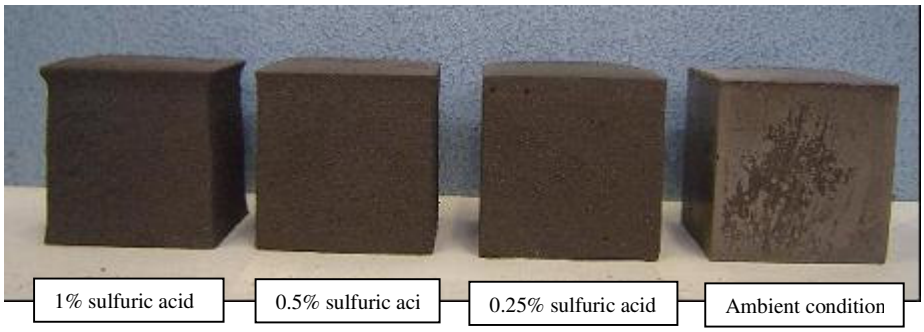

Figure 4.43 Visual Appearance of Geopolymer Mortar Specimens after One Year Exposure in Sulfuric Acid Solution

The visual inspection of the broken pieces of concrete cylinders after the compression test revealed that the acid damage of the specimens, soaked in 2% sulphuric acid solution for one year, seems to have occurred in the outer 20 mm shell of the 100 mm diameter test cylinders (Figure 4.44).

Figure 4.44 Damage to Test Cylinders Exposed to 2% Sulfuric Acid Solution

4.6.2. Test on Concrete Specimens

For the change in compressive strength test, 100x200 mm geopolymer concrete cylinders were soaked in 2%, 1%, and 0.5% concentrations of sulfuric acid. For

change in mass test, the specimens were soaked only in 2% concentration of sulfuric acid, the highest among the three chosen concentrations.

Figure 4.45 shows the change in mass after sulfuric acid exposure up to a period of one year. The test results show that there is a slight mass gain during the first week of exposure due to the mass of solution absorbed by the concrete, as also indicated by the change in mass of specimens soaked in water (Figure 4.36). The mass loss shown in Figure 4.45 is about 3% after one year of exposure. However, by taking into account the mass of absorbed solution, using the rate of water absorption discussed in Section 4.5.3 as a reference, the net mass loss after one year of exposure could be around 5% of the initial mass before soaking. This mass loss is considerably smaller that of Portland cement concrete. By exposing to 5% sulfuric acid and hydrochloric acid, Davidovits (1994b) reported that geopolymeric cements remained stable in acidic environment with mass loss in the range of 5-8%, compared to 30 to 60% mass loss of calcium-aluminate cement and total destruction of Portland cements. The period of exposure was not stated in the work. Song et al (2005a) also showed the superiority of fly ash-based geopolymer concrete in acidic environment compared to Portland cement concrete. By exposing the concrete to 10% sulfuric acid solution, it was found that the mass loss of fly ash-based geopolymer concrete was less than 3% after 56 days of exposure while the Portland cement concrete lost 41% of the mass after just 28 days of exposure. Gourley and Johnson (2005) also reported similar results by using a repeated immersion test in sulfuric acid with pH=1. After about 30 cycles, the geopolymer concrete lost only less than 2% of mass while the Portland cement concrete had about 11% mass loss.

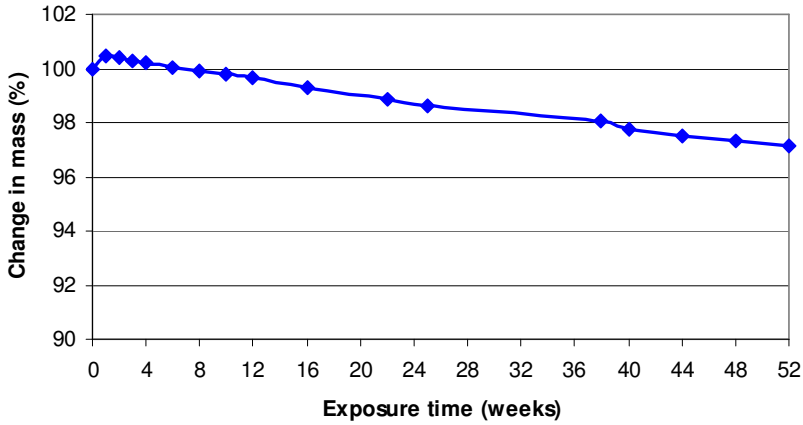

Figure 4.45 Change in Mass of Geopolymer Concrete Exposed to 2% Concentration of Sulfuric Acid Solution

Figures 4.46 to 4.48 show the change in compressive strength of geopolymer concrete for three different concentrations of sulfuric acid solution. Each of these Figures presents the compressive strength of geopolymer concrete after 4 weeks, 12 weeks, 24 weeks and 52 weeks of acid exposure, and compares these results with reference to the compressive strength of unexposed specimens tested one week after casting. The specimens exposed to 2% of sulfuric acid solution were made using a different batch of concrete for each exposure period and, therefore, there were minor variations in the reference compressive strength from batch to batch. The specimens exposed to 1% or 0.5% sulfuric acid solution were made using the same batch for all the exposure periods.

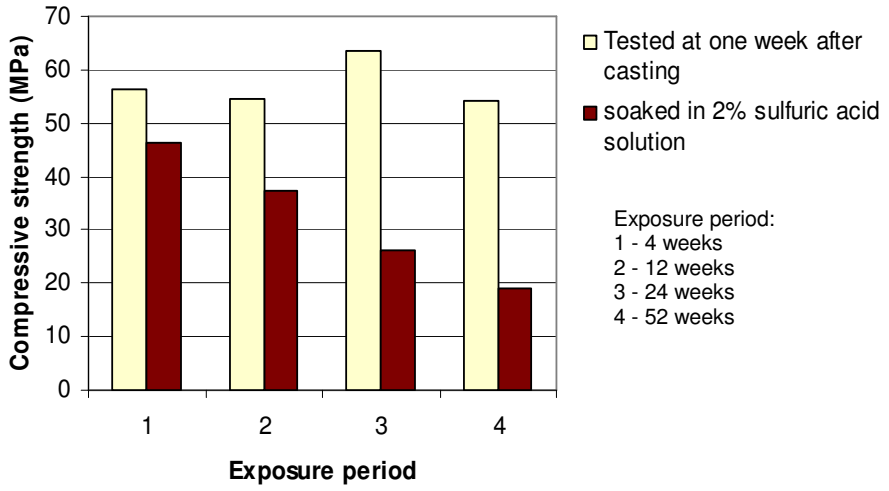

Figure 4.46 Compressive Strength of Geopolymer Concrete Exposed to 2% Sulfuric Acid Solution

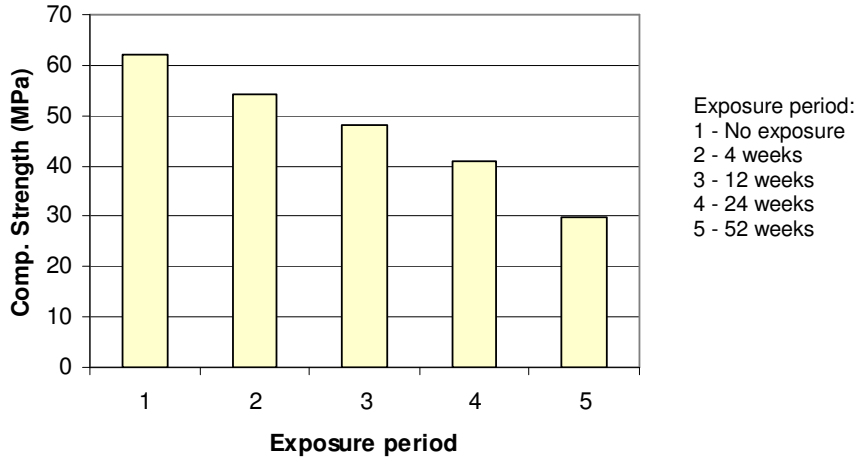

Figure 4.47 Compressive Strength of Geopolymer Concrete Exposed to 1% Sulfuric Acid Solution

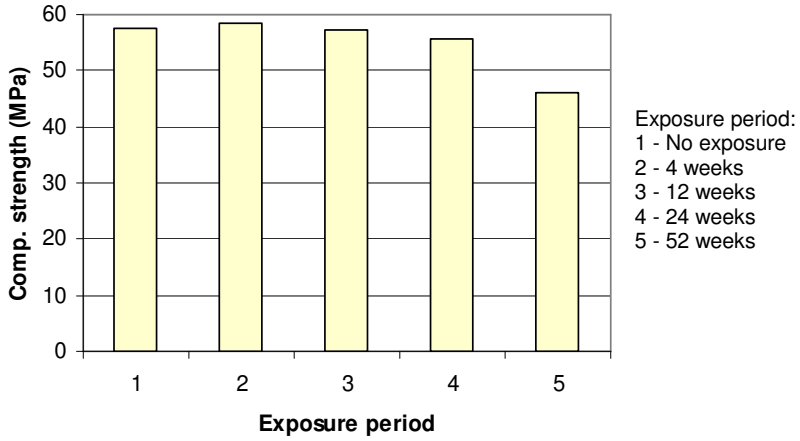

Figure 4.48 Compressive Strength of Geopolymer Concrete Exposed to 0.5% Sulfuric Acid Solution

Figure 4.49 summarises the test data presented in Figures 4.46 to 4.48 in terms of the residual compressive strength of geopolymer concrete after acid exposure as a percentage of the 7th day compressive strength of unexposed specimens.

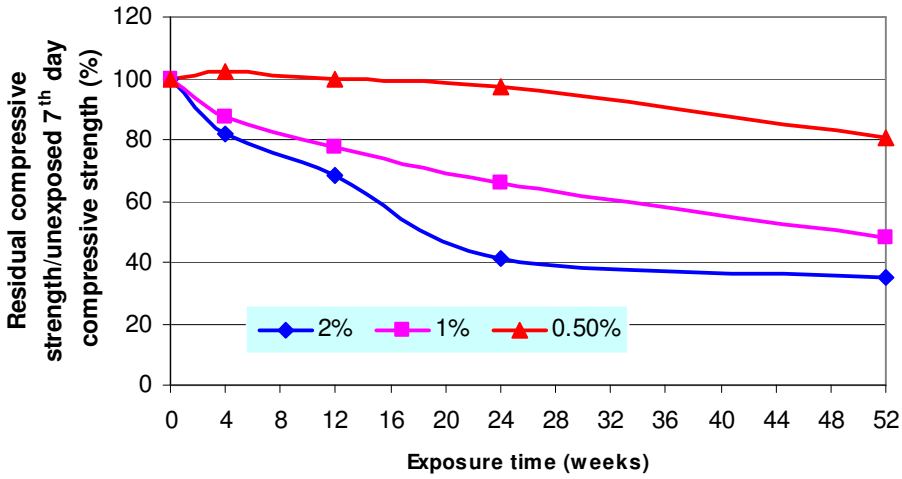

Figure 4.49 Residual Compressive Strength of Geopolymer Concrete after Exposure to Sulfuric Acid Solution

It can be seen from Figure 4.49 that the degradation in the compressive strength of geopolymer concrete due to sulfuric acid exposure depends on the concentration of the acid solution and the period of exposure. The degradation in compressive strength increased as the concentration of the acid solution and the period of

exposure increased. For geopolymer concrete exposed to 2% sulfuric acid solution, the rate of degradation was fast during the first six months but after that the change was not significant up to one year of exposure. A relatively constant rate of strength degradation throughout the exposure period was observed for geopolymer concrete exposed to 1% sulfuric acid solution. On the other hand, for geopolymer concrete exposed to 0.5% sulfuric acid solution, the change in compressive strength during the first six months of exposure was negligible but the degradation became significant between the exposure periods of six months and one year. For the geopolymer concrete exposed to 0.5% concentration of sulphuric acid solution the compressive strength decreased about 20% after one year exposure. This value was about 52% and 65% respectively for geopolymer concrete exposed to 1% and 2% concentration.

The degradation in compressive strength of geopolymeric materials exposed to sulfuric acid solution was also reported by Song et al (2005a) and Bakharev (2005c). Song et al noted that the reduction in compressive strength was in the range of 32 to 37% after 56 days of exposure to 10% sulfuric acid solution. Bakharev suggested that the degradation in strength is related to depolymerisation of aluminosilicate polymers in acidic media and the formation of zeolites.

The acid resistance of geopolymer concrete must be considered in relation to the performance of Portland cement concrete in a similar environment. Past research data have shown that geopolymeric materials perform much better in acid resistance compared to Portland cement (Davidovits 1994, Song et al 2005, Gourley and Johnson 2005). The better performance of geopolymeric materials than that of Portland cement in acidic environment might be attributed to the lower calcium content of the source material as a main possible factor since geopolymer concrete does not rely on lime like Portland cement concrete. Some studies have been reported on better performance in acidic environment of concrete containing lower calcium content than Portland cement. Bakharev (2003) reported the resistance of alkali-activated slag (AAS) concrete to acid attack. It was found that AAS concrete with about 40% CaO performed better than Portland cement concrete with 65% of CaO. The reduction in compressive strength of AAS concrete was about 33% compared to 47% strength reduction of Portland cement concrete. Chang et al (2005) studied the acid resistance of Portland cement concretes with various supplementary

cementitious materials. They observed that concretes produced by mixing Portland cement with silica fume and fly ash had the lowest calcium content and, therefore, performed the best among the other mixtures in acidic environment.

4.6.3. Tests on Mortar Specimens

The geopolymer mortar test specimens (75 mm cubes) were exposed to 1%, 0.5%, and 0.25% concentrations of sulfuric acid solution and the change in compressive strength was determined. The change in mass was determined only for the highest concentration (1%). The purpose of these tests was to evaluate the effect of the coarse aggregate on the aid resistance of fly ash-based geopolymer concrete.

The average 7th day compressive strength of mortar cubes was 41 MPa with a standard deviation of 4 MPa. The average unit weight was 2015 kg/m^3 with a standard deviation of 75 kg/m^3.

Figure 4.50 presents the change in mass of geopolymer mortar cubes for exposure periods up to one year. The mass loss after one year of exposure was about 1.5%, but the net mass loss would be slightly higher after allowing for the mass of absorbed solution.

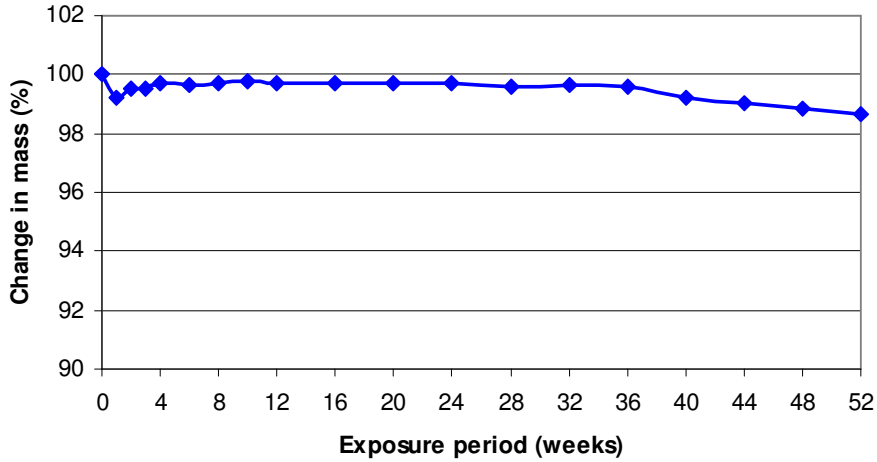

Figure 4.50 Change in Mass of Geopolymer Mortar Cubes Exposed to 1% Concentration of Sulfuric Acid Solution

Figure 4.51 presents the change in compressive strength of geopolymer mortar cubes exposed to the different concentrations of sulfuric acid solution with reference to the average 7th day compressive strength of unexposed specimens.

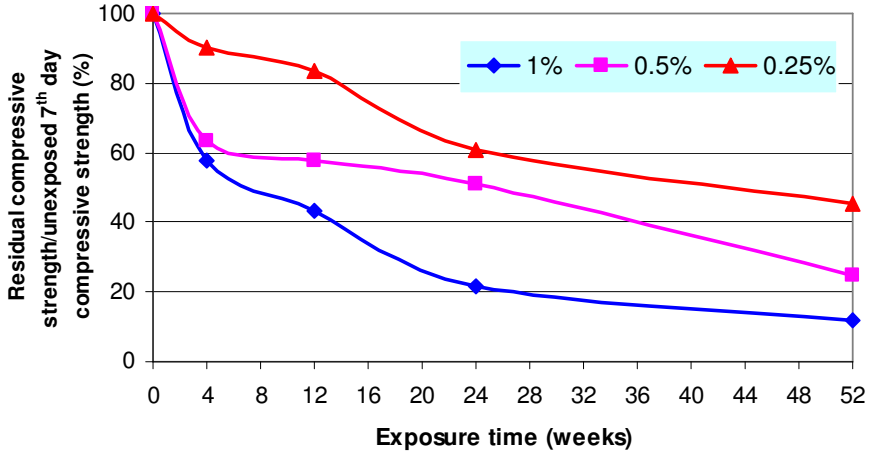

Figure 4.51 Residual Compressive Strength of Geopolymer Mortar Cubes Exposed to Various Concentrations of Sulfuric Acid Solution

As for the geopolymer concrete specimens, there was degradation in the compressive strength of geopolymer mortar cubes exposed to sulfuric acid solution. The general trends of test data presented in Figure 4.51 are similar those shown in Figure 4.49. However, the extent of degradation in compressive strength of mortar specimens was larger compared to that of concrete specimens. The decrease in the compressive strength of geopolymer mortar cubes after one year of exposure was about 55%, 75% and 88% for acid solution concentration of 0.25, 0.5% and 1% respectively.

The test results suggest that the degradation in the compressive strength is mainly due to the degradation of the geopolymer matrix rather than the aggregates. Since the mortar contained about 50% (by mass) of binder, when compared to about 23% (by mass) of binder in the concrete, the extent of degradation in the compressive strength of mortar was larger than that of concrete. It appears that the percentage mass of aggregates in a mixture influence the sulfuric acid resistant of geopolymer concrete, in addition to the effect of type of aggregates as observed by Song et. al(2005b).

CHAPTER 5:
CONCLUSIONS

5.1. Introduction

This Chapter presents a brief summary of the study and a set of conclusions.

In this work, the long-term properties of low-calcium fly ash-based geopolymer concrete were studied. The long-term properties included in the study were creep, drying shrinkage, sulfate resistance, and sulfuric acid resistance.

Fly ash-based geopolymer concrete in this study utilised the low-calcium (ASTM Class F) dry fly ash as the source material. The alkaline liquid comprised a combination of sodium silicate solution and sodium hydroxide solids in flakes or pellets form dissolved in water. Coarse and fine aggregates used in the local concrete industry were used. The coarse aggregates were crushed granite-type aggregates comprising 20 mm, 14 mm and 7 mm and the fine aggregate was fine sand. High range water reducer super plasticiser was used to improve the workability of fresh geopolymer concrete.

The mixture proportions used in this study were developed based on previous study on fly ash-based geopolymer concrete (Hardjito and Rangan, 2005). Two different mixtures, Mixture-1 and Mixture-2, were used for the concrete specimens and one mixture for the mortar specimens. The average compressive strength of Mixture-1 was around 60 MPa and that of Mixture-2 was about 40 MPa.

Tests specimens were manufactured in the laboratory using the equipments normally used for Portland cement concrete, such as a pan mixer, steel moulds and vibrating table. The aggregates were first mixed with the fly ash in the pan mixer for about 3 minutes. The alkaline liquid was mixed with the super plasticiser and extra water (if any). The liquid component of the mixture was then added to the dry mix and the mixing continued for another 4 minutes. The fresh concrete was then cast into the moulds in three layers for cylindrical specimens or two layers for prismatic specimens. The specimens were compacted layer by layer by using 60 to 80 manual

strokes by a rodding bar, followed by vibration on a vibrating table for 12 to 15 seconds.

After casting, most of the specimens were heat-cured at 60^{o}C for 24 hours. Some specimens were cured in ambient conditions of the laboratory. For heat-curing, either steam curing or dry (oven) curing was used.

Test procedures used in this study were based on available or modified procedures normally used for Portland cement concrete either from the available standards such as the Australian Standard or ASTM, or from the previously published works in the areas within this study.

The creep behaviour of fly-ash based geopolymer concrete was studied for both Mixture-1 and Mixture-2. For each mixture, 150x300 mm cylinders were made. The test specimens were heat-cured either in the oven or in the steam-curing chamber. The specimens were loaded on the 7th day after casting. The sustained stress on the specimens was about 40 percent of the 7th day compressive strength. The creep tests were conducted up to a period of one year.

As in the case of creep test, Mixture-1 and Mixture-2 were also used to study the drying shrinkage behaviour of heat-cured geopolymer concrete. In addition, a series of specimens made from Mixture-1 were cured in ambient conditions of the laboratory, without any heat-curing. The shrinkage test specimens were 75x75x285 mm prisms for drying shrinkage test and 100x200 mm cylinders for compressive strength test. For heat-cured specimens the drying shrinkage was observed for the period up to one year, while for ambient-cured specimens it was observed only up to three months period. The initial measurement, considered as age 'zero', took place on the 3rd day after casting the specimens.

For sulfate resistance tests, only Mixture-1 was used. The test specimens were immersed in 5% sodium sulfate solution for various periods of exposure up to one year. The sulfate resistance was evaluated based on the change in mass, change in length and change in compressive strength of the specimens after sulfate exposure.

The test specimens were 100x200 mm cylinders for change in mass and change in compressive strength tests and 75x75x285 mm prisms for change in length test.

The sulfuric acid resistance of fly ash-based geopolymer concrete was studied for Mixture-1. In addition, the sulfuric acid resistance test was also conducted on geopolymer mortar specimens to study the effect of the coarse aggregates on the acid resistance of fly ash-based geopolymer concrete. The concentration of sulfuric acid solution was 2%, 1% and 0.5% for soaking concrete specimens and 1%, 0.5% and 0.25% for soaking mortar specimens. The sulfuric acid resistance of geopolymer concrete and geopolymer mortar was evaluated based on the mass loss and the residual compressive strength of the test specimens after acid exposure up to one year. The test specimens were 100x200 mm cylinders for concrete specimens and 75 mm cubes for mortar specimens.

For each type of test, companion specimens were prepared and tested to determine the 7^{th} day compressive strength. As the 7^{th} day compressive strength did not change significantly, this value was used as a standard or reference compressive strength to which the other values of compressive strength were compared.

Calculations were performed to predict the creep and drying shrinkage of geopolymer concrete using Gilbert (2002) method incorporated in the draft version of the forthcoming Australian Standard for Concrete Structures AS3600 (2005). The test results were compared with the calculated values.

5.2. Conclusions

Based on the test results, the following conclusions are drawn:

1. There is no substantial gain in the compressive strength of heat-cured fly ash-based geopolymer concrete with age.
2. Fly ash-based geopolymer concrete cured in the laboratory ambient conditions gains compressive strength with age. The 7^{th} day compressive strength of ambient-cured specimens depends on the average ambient temperature during the first week after casting; higher the average ambient temperature higher is the compressive strength.

3. Heat-cured fly ash-based geopolymer concrete undergoes low creep. The specific creep, defined as the creep strain per unit stress, after one year ranged from 15 to 29 x 10^{-6}/MPa for the corresponding compressive strength of 67 MPa to 40 MPa.
4. The creep coefficient, defined as the ratio of creep strain-to-instantaneous strain, after one year for heat-cured geopolymer concrete with compressive strength of 40, 47 and 57 MPa is around 0.6 to 0.7; for geopolymer concrete with compressive strength of 67 MPa this value is around 0.4 to 0.5. These values are about 50% of those experienced by Portland cement concrete, as predicted by Gilbert method given in the draft Australian Standard for Concrete Structures AS3600 (2005).
5. The heat-cured fly ash-based geopolymer concrete undergoes very little drying shrinkage in the order of about 100 micro strains after one year. This value is significantly smaller than the range of values of 500 to 800 micro strain for Portland cement concrete, as predicted by Gilbert method given in the draft Australian Standard for Concrete Structures AS3600 (2005).
6. The drying shrinkage strain of ambient-cured specimens is in the order of 1500 microstrains after three months. This value is many folds larger than that of heat-cured specimens, and the most part of that occurs during the first few weeks.
7. The test results demonstrate that heat-cured fly ash-based geopolymer concrete has an excellent resistance to sulfate attack. There is no damage to the surface of test specimens after exposure to sodium sulfate solution up to one year. There are no significant changes in the mass and the compressive strength of test specimens after various periods of exposure up to one year. These test observations indicate that there is no mechanism to form gypsum or ettringite from the main products of polymerisation in heat-cured low-calcium fly ash-based geopolymer concrete.
8. Exposure to sulfuric acid solution damages the surface of heat-cured geopolymer concrete test specimens and causes a mass loss of about 3% after one year of exposure. The severity of the damage depends on the acid concentration.
9. The sulfuric acid attack also causes degradation in the compressive strength of heat-cured geopolymer concrete; the extent of degradation depends on the concentration of the acid solution and the period of exposure. However, the sufuric acid resistance of heat-cured geopolymer concrete is significantly better than that of Portland cement concrete as reported in earlier studies.

10. The tests on heat-cured geopolymer mortar specimens indicate that the degradation in the compressive strength due to sulfuric acid attack is mainly due to the degradation in the geopolymer matrix rather than the aggregates. The degradation in compressive strength of mortar specimens is larger than that of concrete specimens due to the larger geopolymer matrix content by mass of mortar specimens.

REFERENCES

Bakharev, T., Sanjayan, J. G., & Cheng, J. B. (2003). Resistance of alkali-activated slag concrete to acid attack. *Cement and Concrete Research, 33*, 1607-1611.

Bakharev, T. (2005a). Durability of geopolymer materials in sodium and magnesium sulfate solutions. *Cement And Concrete Research, 35*(6), 1233-1246.

Bakharev, T. (2005b). Geopolymeric materials prepared using Class F fly ash and elevated temperature curing. *Cement And Concrete Research, 35*(6), 1224-1232.

Bakharev, T. (2005c). Resistance of geopolymer materials to acid attack. *Cement And Concrete Research, 35*(4), 658-670.

Balaguru, P., Kurtz, S., & Rudolph, J. (1997). *Geopolymer for Repair and Rehabilitation of Reinforced Concrete Beams*. The Geopolymer Institute. Retrieved 3 April, 2002, from the World Wide Web: www.geopolymer.org

Cheng, T. W., & Chiu, J. P. (2003). Fire-resistant geopolymer produced by granulated blast furnace slag. *Minerals Engineering, 16*(3), 205-210.

Comrie, D. C., Paterson, J. H., & Ritchey, D. J. (1988). *Geopolymer Technologies in Toxic Waste Management.* Paper presented at the Geopolymer '88, First European Conference on Soft Mineralurgy, Compiegne, France.

Davidovits, J. (1984). Synthetic Mineral Polymer Compound of The Silicoaluminates Family and Preparation Process, *United States Patent - 4,472,199* (pp. 1-12). USA.

Davidovits, J. (1988a). *Soft Mineralurgy and Geopolymers.* Paper presented at the Geopolymer '88, First European Conference on Soft Mineralurgy, Compiegne, France.

Davidovits, J. (1988b). *Geopolymer Chemistry and Properties.* Paper presented at the Geopolymer '88, First European Conference on Soft Mineralurgy, Compiegne, France.

Davidovits, J. (1988c). *Geopolymers of the First Generation: SILIFACE-Process.* Paper presented at the Geopolymer '88, First European Conference on Soft Mineralurgy, Compiegne, France.

Davidovits, J. (1988d). *Geopolymeric Reactions in Archaeological Cements and in Modern Blended Cements.* Paper presented at the Geopolymer '88, First European Conference on Soft Mineralurgy, Compiegne, France.

Davidovits, J. (1991). Geopolymers: Inorganic Polymeric New Materials. *Journal of Thermal Analysis, 37*, 1633-1656.

Davidovits, J. (1994a). *High-Alkali Cements for 21st Century Concretes.* Paper presented at the V. Mohan Malhotra Symposium on Concrete Technology: Past, Present And Future, University of California, Berkeley.

Davidovits, J. (1994b). Properties of Geopolymer Cements. In Kiev (Ed.), *First International Conference on Alkaline Cements and Concretes* (pp. 131-149). Kiev, Ukraine: Kiev State Technical University.

Davidovits, J. (1994c). Global Warming Impact on the Cement and Aggregates Industries. *World Resource Review, 6*(2), 263-278.

Davidovits, J. (1999, 30 June - 2 July 1999). *Chemistry of Geopolymeric Systems, Terminology.* Paper presented at the Geopolymere '99 International Conference, Saint-Quentin, France.

Davidovits, J. (2005). *Green-Chemistry and Sustainable Development Granted and False Ideas About Geopolymer-Concrete.* Paper presented at the International Workshop on Geopolymers and Geopolymer Concrete (GGC), Perth, Australia.

Fernández-Jiménez, A., & Palomo, A. (2003). Characterisation of fly ashes. Potential reactivity as alkaline cements. *Fuel, 82*(18), 2259-2265.

Gilbert, R. I. (1988). *Time Effects in Concrete Structures*. Amsterdam: Elsevier.

Gilbert, R. I. (2002). Creep and shrinkage models for high strength concrete - proposal for inclusion in AS3600. *Australian Journal of Structural Engineering, 4*(2), 95-106.

Gourley, J. T. (2003). *Geopolymers; Opportunities for Environmentally Friendly Construction Materials.* Paper presented at the Materials 2003 Conference: Adaptive Materials for a Modern Society, Sydney.

Gourley, J. T., & Johnson, G. B. (2005). *Developments in Geopolymer Precast Concrete.* Paper presented at the International Workshop on Geopolymers and Geopolymer Concrete, Perth, Australia.

Hardjito, D., Wallah, S. E., & Rangan, B. V. (2002a). *Research Into Engineering Properties of Geopolymer Concrete.* Paper presented at the Geopolymer 2002 International Conference, Melbourne.

Hardjito, D., Wallah, S. E., & Rangan, B. V. (2002b). Study on Engineering Properties of Fly Ash-Based Geopolymer Concrete. *Journal of the Australasian Ceramic Society, 38*(1), 44-47.

Hardjito, D., Wallah, S. E., Sumajouw, D. M. J., & Rangan, B. V. (2003). *Geopolymer Concrete: Turn Waste Into Environmentally Friendly Concrete.* Paper presented at the International Conference on Recent Trends in Concrete Technology and Structures (INCONTEST), Coimbatore, India.

Hardjito, D., Wallah, S. E., Sumajouw, D. M. J., & Rangan, B. V. (2004a). *Properties of Geopolymer Concrete with Fly Ash as Source Material: Effect of Mixture Composition.* Paper presented at the Seventh CANMET/ACI International Conference on Recent Advances in Concrete Technology, Las Vegas, USA.

Hardjito, D., Wallah, S. E., Sumajouw, D. M. J., & Rangan, B. V. (2004b). On the Development of Fly Ash-Based Geopolymer Concrete. *ACI Materials Journal, 101*(6), 467-472.

Hardjito, D., & Rangan, B. V. (2005). *Development and Properties of Low-Calcium Fly Ash-Based Geopolymer Concrete*. Research Report GC1, Perth, Australia: Faculty of Engineering, Curtin University of Technology.

Hardjito, D., Wallah, S. E., Sumajouw, D. M. J., & Rangan, B. V. (2005a). Fly Ash-Based Geopolymer Concrete. *Australian Journal of Structural Engineering, Vol. 6*(1), 77-86.

Hardjito, D., Wallah, S. E., Sumajouw, D. M. J., & Rangan, B. V. (2005b). *Introducing Fly Ash-Based Geopolymer Concrete: Manufacture and Engineering Properties.* Paper presented at the Our World in Concrete and Structures International Conference, Singapore.

Hime, W. G. (2003). Comments on Geopolymer Concrete, Private Communication.

Lea, F. M. (1970). *The Chemistry of Cement and Concrete*. London: Edward Arnold.

Li, G., & Zhao, X. (2003). Properties of concrete incorporating fly ash and ground granulated blast-furnace slag. *Cement & Concrete Composites, 25*(3), 293-299.

Malhotra, V. M. (1999). Making Concrete "Greener" With Fly Ash. *ACI Concrete International, 21*(5), 61-66.

Malhotra, V. M., & Mehta, P. K. (2002). *High-Performance, High-Volume Fly Ash Concrete: Materials, Mixture Proportioning, Properties, Construction Practice, and Case Histories*. Ottawa: Supplementary Cementing Materials for Sustainable Development Inc.

Malone, P. G., Charlie A. Randall, J., & Kirkpatrick, T. (1985). *Potential Applications of Alkali-Activated Alumino-Silicate Binders in Military Operations*. Washington, DC: Department of The Army, Assistant Secretary of the Army (R&D).

McCaffrey, R. (2002). Climate Change and the Cement Industry. *Global Cement and Lime Magazine (Environmental Special Issue)*, 15-19.

Mehta, P. K. (1983). Mechanism of Sulfate Attack on Portland Cement Concrete-Another Look. *Cement and Concrete Research, 13*(3), 401-406.

Mehta, P. K. (1985). Studies on Chemical Resistance of Low Water/Cement Ratio Concretes. *Cement and Concrete Research, 15*(6), 969-978.

Neville, A. M., Dilger, W. H., & Brooks, J. J. (1983). *Creep of plain and structural concrete*. London: Construction Press, Longman Group.

Neville, A. M. (2000). *Properties of Concrete* (Fourth and Final ed.). Essex, England: Pearson Education, Longman Group.

Palomo, A., M.W.Grutzeck, & M.T.Blanco. (1999). Alkali-activated fly ashes A cement for the future. *Cement And Concrete Research, 29*(8), 1323-1329.

Phair, J. W., & van Deventer, J. S. J. (2001). Effect of silicate activator pH on the leaching and material characteristics of waste-based inorganic polymers. *Minerals Engineering, 14*(3), 289-304.

Phair, J. W., & van Deventer, J. S. J. (2002). Effect of the silicate activator pH on the microstructural characteristics of waste-based geopolymers. *International Journal of Mineral Processing, 66*(1-4), 121-143.

Rangan, B. V., Hardjito, D., Wallah, S. E., & Sumajouw, D. M. J. (2005a). Fly ash-based geopolymer concrete: a construction material for sustainable development. *Concrete in Australia, 31,* 25-30.

Rangan, B. V., Hardjito, D., Wallah, S. E., & Sumajouw, D. M. J. (2005b). *Studies of fly ash-based geopolymer concrete.* Paper presented at the World Congress Geopolymer 2005, Saint-Quentin, France.

Roy, D. M. (1999). Alkali-activated cements Opportunities and Challenges. *Cement & Concrete Research, 29*(2), 249-254.

Song, X. J., Marosszeky, Brungs, M. M., & Munn, R. (2005a, 17-20 April). *Durability of fly ash-based Geopolymer concrete against sulphuric acid attack.* Paper presented at the 10DBMC International Conference on Durability of Building Materials and Components, Lyon, France.

Song, X.-J., Munn, R., Marosszeky, M., & Brungs, M. (2005b). *Investigation of Cracking Developed in Sulphuric Acid Resistant Concretes.* Paper presented at the CIA 22nd Biennial Conference, Concrete 05, Melbourne, Australia.

Standards-ASTM. (1993). Standard Test Method for Length Change of Hardened Hydraulic-Cement Mortar and Concrete. *C 157 - 93*.

Standards-ASTM. (1995). Standard Test Method for Length Change of Hydraulic-Cement Mortars Exposed to a Sulfate Solution. *C 1012 - 95a*.

Standards-ASTM. (1997). Use of Apparatus for the Determination of Length Change of Hardened Cement Paste, Mortar, and Concrete. *C 490 - 97*.

Standards-Australia. (1992). Methods of testing concrete - Determination of the drying shrinkage of concrete for samples prepared in the field or in the laboratory. *AS 1012.13 - 1992*.

Standards-Australia. (1996a). Methods of testing concrete - Determination of creep of concrete cylinders in compression. *AS 1012.16-1996*.

Standards-Australia. (1996b). Method of testing portland and blended cements - Length change of portland and blended cement mortars exposed to a sulfate solution. *AS 2350.14-1996*.

Standards-Australia. (1999). Methods of testing concrete - Determination of the compressive strength of concrete specimens. *AS 1012.9-1999*.

Standards-Australia. (2005). Concrete Structures. *Draft for Public Comment (Revision of AS 3600 - 2001).*

Swanepoel, J. C., & Strydom, C. A. (2002). Utilisation of fly ash in a geopolymeric material. *Applied Geochemistry, 17*(8), 1143-1148.

Tikalsky, P. J., & Carrasquillo, R. L. (1992). Influence of Fly Ash on the Sulfate Resistance of Concrete. *ACI Materials Journal, 89*(1), 69-75.

Torii, K., Taniguchi, K., & Kawamura, M. (1995). Sulfate Resistance of High Fly Ash Content Concrete. *Cement And Concrete Research, 25*(4), 759-768.

van Jaarsveld, J. G. S., van Deventer, J. S. J., & Lorenzen, L. (1997). The potential use of geopolymeric materials to immobilise toxic metals: Part I. Theory and applications. *Minerals Engineering, 10*(7), 659-669.

van Jaarsveld, J. G. S., van Deventer, J. S. J., & Schwartzman, A. (1999). The potential use of geopolymeric materials to immobilise toxic metals: Part II. Material and leaching characteristics. *Minerals Engineering, 12*(1), 75-91.

van Jaarsveld, J. G. S., van Deventer, J. S. J., & Lukey, G. C. (2002a). The effect of composition and temperature on the properties of fly ash- and kaolinite-based geopolymers. *Chemical Engineering Journal, 89*(1-3), 63-73.

van Jaarsveld, J. G. S., van Deventer, J. S. J., & Lukey, G. C. (2002b). The characterisation of source materials in fly ash-based geopolymers. *Materials Letters, 3975*(Article in press).

van Jaarsveld, J. G. S., van Deventer, J. S. J., & Lukey, G. C. (2003). The characterisation of source materials in fly ash-based geopolymers. *Materials Letters, 57*(7), 1272-1280.

Warner, R. F., Rangan, B. V., Hall, A. S., & Faulkes, K. A. (1998). *Concrete Structures*. Melbourne: Longman.

Wee, T. H., Suryavanshi, A. K., Wong, S. F., & Rahman, A. K. M. A. (2000). Sulfate Resistance of Concrete Containing Mineral Admixtures. *ACI Materials Journal, 97*(5), 536-549.

Xu, H., & Deventer, J. S. J. V. (1999). *The Geopolymerisation of Natural Alumino-Silicates.* Paper presented at the Geopolymere '99 International Conference, Saint-Quentin, France.

Xu, H., & Deventer, J. S. J. V. (2000). The geopolymerisation of alumino-silicate minerals. *International Journal of Mineral Processing, 59*(3), 247-266.

APPENDIX A

Creep Strain Calculations by Gilbert's Method

Creep Prediction - Gilbert's Method		(1CR)
Compressive strength (MPa)	f'_c	67
Elastic strain (microstrain)	ε_{ce}	902
Hypothetical thickness (mm)	t_h	75
Interior environment	k_4	0.65
Basic creep coefficient	$\varphi_{cc.b}$	1.96
	f_{cm}/f'_c	1
Maturity coefficient	k_3	1.1
	α_2	1.615
	α_3	0.667
	k_5	0.887

t (days)	k_2	$\varphi_{cc(t)}$	$\varepsilon_{cc(t)}$	$\varepsilon_{cc} + \varepsilon_{ce}$
			(x 10^{-6})	(x 10^{-6})
0	0.000	0.000	0	902
0.083	0.019	0.024	22	924
0.25	0.046	0.057	52	954
1	0.132	0.164	148	1050
2	0.216	0.269	243	1145
3	0.285	0.354	319	1222
4	0.343	0.426	384	1287
5	0.393	0.489	441	1344
6	0.438	0.545	492	1394
7	0.479	0.595	537	1440
14	0.684	0.849	767	1669
21	0.813	1.011	912	1815
28	0.906	1.126	1016	1918
42	1.031	1.282	1157	2059
56	1.114	1.384	1249	2152
70	1.174	1.458	1316	2219
84	1.219	1.515	1367	2269
112	1.283	1.595	1439	2342
147	1.337	1.662	1500	2402
168	1.361	1.691	1526	2429
196	1.386	1.722	1554	2457
231	1.411	1.753	1582	2485
252	1.423	1.768	1596	2498
280	1.437	1.785	1611	2514
308	1.448	1.800	1624	2527
336	1.458	1.812	1636	2538
364	1.467	1.823	1645	2548

Creep Prediction - Gilbert's Method		(2CR)
Compressive strength (MPa)	f'_c	57
Elastic strain (microstrain)	ε_{ce}	851
Hypothetical thickness (mm)	t_h	75
Interior environment	k_4	0.65
Basic creep coefficient	$\varphi_{cc.b}$	2.213
	f_{cm}/f'_c	1
Maturity coefficient	k_3	1.1
	α_2	1.615
	α_3	0.667
	k_5	0.953

t (days)	k_2	$\varphi_{cc(t)}$	$\varepsilon_{cc(t)}$	$\varepsilon_{cc} + \varepsilon_{ce}$
			(x 10^{-6})	(x 10^{-6})
0	0.000	0.000	0	851
0.083	0.019	0.029	25	876
0.25	0.046	0.069	59	910
1	0.132	0.199	169	1020
2	0.216	0.326	278	1129
3	0.285	0.430	366	1217
4	0.343	0.517	440	1291
5	0.393	0.594	505	1356
6	0.438	0.661	563	1414
7	0.479	0.723	615	1466
14	0.684	1.031	878	1729
21	0.813	1.227	1045	1896
28	0.906	1.367	1163	2015
42	1.031	1.556	1324	2176
56	1.114	1.681	1431	2282
70	1.174	1.771	1507	2358
84	1.219	1.839	1565	2416
112	1.283	1.936	1648	2499
147	1.337	2.017	1717	2568
168	1.361	2.053	1747	2599
196	1.386	2.091	1780	2631
231	1.411	2.128	1812	2663
252	1.423	2.147	1827	2678
280	1.437	2.167	1845	2696
308	1.448	2.185	1860	2711
336	1.458	2.200	1873	2724
364	1.467	2.214	1884	2735

Creep Prediction - Gilbert's Method		(3CR)
Compressive strength (MPa)	f'_c	47
Elastic strain (microstrain)	ε_{ce}	828
Hypothetical thickness (mm)	t_h	75
Interior environment	k_4	0.65
Basic creep coefficient	$\varphi_{cc.b}$	2.52
	f_{cm}/f'_c	1
Maturity coefficient	k_3	1.1
	α_2	1.615
	α_3	0.667
	k_5	1.0

t (days)	k_2	$\varphi_{cc(t)}$	$\varepsilon_{cc(t)}$	$\varepsilon_{cc} + \varepsilon_{ce}$
			(x 10^{-6})	(x 10^{-6})
0	0.000	0.000	0	829
0.083	0.019	0.035	29	858
0.25	0.046	0.083	69	897
1	0.132	0.237	197	1025
2	0.216	0.390	323	1152
3	0.285	0.513	425	1254
4	0.343	0.618	512	1340
5	0.393	0.709	587	1416
6	0.438	0.790	654	1483
7	0.479	0.863	715	1543
14	0.684	1.232	1020	1849
21	0.813	1.466	1214	2043
28	0.906	1.632	1352	2181
42	1.031	1.858	1540	2368
56	1.114	2.007	1663	2492
70	1.174	2.114	1752	2581
84	1.219	2.196	1819	2648
112	1.283	2.312	1916	2745
140	1.328	2.393	1983	2811
168	1.361	2.452	2031	2860
196	1.386	2.497	2069	2898
224	1.406	2.534	2099	2928
252	1.423	2.563	2124	2953
280	1.437	2.588	2145	2973
308	1.448	2.609	2162	2991
336	1.458	2.628	2177	3006
364	1.467	2.644	2190	3019

Creep Prediction - Gilbert's Method		(4CR)
Compressive strength (MPa)	f'_c	40
Elastic strain (microstrain)	ε_{ce}	761
Hypothetical thickness (mm)	t_h	75
Interior environment	k_4	0.65
Basic creep coefficient	$\varphi_{cc.b}$	2.8
	f_{cm}/f'_c	1
Maturity coefficient	k_3	1.1
	α_2	1.615
	α_3	0.667
	k_5	1.0

t (days)	k_2	$\varphi_{cc(t)}$	$\varepsilon_{cc(t)}$	$\varepsilon_{cc} + \varepsilon_{ce}$
			(x 10^{-6})	(x 10^{-6})
0	0.000	0.000	0	761
0.083	0.019	0.039	30	791
0.25	0.046	0.092	70	832
1	0.132	0.264	201	962
2	0.216	0.433	330	1091
3	0.285	0.570	434	1195
4	0.343	0.686	522	1284
5	0.393	0.788	600	1361
6	0.438	0.878	668	1430
7	0.479	0.959	730	1491
14	0.684	1.368	1042	1803
21	0.813	1.629	1240	2001
28	0.906	1.814	1381	2142
42	1.031	2.065	1572	2333
56	1.114	2.230	1698	2460
70	1.174	2.349	1789	2550
84	1.219	2.440	1858	2619
112	1.283	2.569	1956	2718
140	1.328	2.659	2024	2786
168	1.361	2.724	2074	2836
196	1.386	2.775	2113	2874
224	1.406	2.815	2144	2905
252	1.423	2.848	2169	2930
280	1.437	2.876	2190	2951
308	1.448	2.899	2208	2969
336	1.458	2.920	2223	2984
364	1.467	2.937	2236	2998

APPENDIX B

Shrinkage Strain Calculations by Gilbert's Method

Shrinkage Prediction - Gilbert's Method	**(1DS)**		
Compressive strength (MPa)	**f'_c**	**65**	
Hypothetical thickness (mm)	**t_h**	**50**	
Interior environment	**k_4**	**0.65**	
Final endogenous shrinkage	**ε_{cse}***	**145**	
Quality of aggregate	**$\varepsilon_{csd.b}$***	**1000**	**$x10^{-6}$, Perth**
Basic drying shrinkage	**$\varepsilon_{csd.b}$**	**480**	**$x10^{-6}$**
	α_1	**1.735**	

t (days)	ε_{cse}	k_1	ε_{csd}	ε_{cs}
	($x10^{-6}$)		($x10^{-6}$)	($x10^{-6}$)
0	0	0.000	0	0
1	14	0.204	64	77
2	26	0.327	102	128
3	38	0.422	132	169
4	48	0.499	156	204
5	57	0.565	176	233
6	65	0.622	194	259
7	73	0.672	210	283
14	109	0.909	284	393
24	132	1.091	340	472
28	136	1.140	356	492
42	143	1.260	393	536
57	145	1.339	418	562
70	145	1.387	433	578
84	145	1.426	445	590
105	145	1.468	458	603
143	145	1.520	474	619
175	145	1.548	483	628
196	145	1.563	488	633
224	145	1.579	493	638
252	145	1.591	497	642
280	145	1.602	500	645
308	145	1.611	503	648
337	145	1.619	505	650
364	145	1.626	507	652

Shrinkage Prediction - Gilbert's Method		**(2DS)**	
Compressive strength (MPa)	**f'_c**	**57**	
Hypothetical thickness (mm)	**t_h**	**50**	
Interior environment	**k_4**	**0.65**	
Final endogenous shrinkage	**ε_{cse}***	**121**	
Quality of aggregate	**$\varepsilon_{csd.b}$***	**1000**	**$x10^{-6}$, Perth**
Basic drying shrinkage	**$\varepsilon_{csd.b}$**	**544**	**$x10^{-6}$**
	α_1	**1.735**	

t (days)	**ε_{cse}**	**k_1**	**ε_{csd}**	**ε_{cs}**
	($x10^{-6}$)		**($x10^{-6}$)**	**($x10^{-6}$)**
0	0	0.000	0	0
1	12	0.204	72	84
2	22	0.327	116	137
3	31	0.422	149	180
4	40	0.499	177	216
5	48	0.565	200	247
6	55	0.622	220	275
7	61	0.672	238	299
14	91	0.909	321	413
24	110	1.091	386	496
28	114	1.140	403	517
42	119	1.260	445	565
57	121	1.339	473	594
70	121	1.387	490	611
84	121	1.426	504	625
105	121	1.468	519	640
143	121	1.520	537	658
175	121	1.548	547	668
196	121	1.563	553	674
224	121	1.579	558	679
252	121	1.591	563	684
280	121	1.602	567	688
308	121	1.611	570	691
337	121	1.619	573	694
364	121	1.626	575	696

Shrinkage Prediction - Gilbert's Method		**(3DS)**	
Compressive strength (MPa)	**f'_c**	**50**	
Hypothetical thickness (mm)	**t_h**	**50**	
Interior environment	**k_4**	**0.65**	
Final endogenous shrinkage	**ε_{cse}***	**100**	
Quality of aggregate	**$\varepsilon_{csd.b}$***	**1000**	**$x10^{-6}$, Perth**
Basic drying shrinkage	**$\varepsilon_{csd.b}$**	**600**	**$x10^{-6}$**
	α_1	**1.735**	

t (days)	ε_{cse}	k_1	ε_{csd}	ε_{cs}
	($x10^{-6}$)		($x10^{-6}$)	($x10^{-6}$)
0	0	0.000	0	0
1	10	0.204	80	89
2	18	0.327	127	146
3	26	0.422	164	190
4	33	0.499	195	228
5	39	0.565	220	260
6	45	0.622	243	288
7	50	0.672	262	312
14	75	0.909	355	430
24	91	1.091	425	516
28	94	1.140	445	539
42	99	1.260	491	590
57	100	1.339	522	622
70	100	1.387	541	641
84	100	1.426	556	656
105	100	1.468	573	673
143	100	1.520	593	693
175	100	1.548	604	704
196	100	1.563	609	709
224	100	1.579	616	716
252	100	1.591	621	721
280	100	1.602	625	725
308	100	1.611	628	728
337	100	1.619	631	731
364	100	1.626	634	734

Shrinkage Prediction - Gilbert's Method		**(4DS)**	
Compressive strength (MPa)	**f'_c**	**41**	
Hypothetical thickness (mm)	**t_h**	**50**	
Interior environment	**k_4**	**0.65**	
Final endogenous shrinkage	**ε_{cse}***	**73**	
Quality of aggregate	**$\varepsilon_{csd.b*}$**	**1000**	**$x10^{-6}$, Perth**
Basic drying shrinkage	**$\varepsilon_{csd.b}$**	**672**	**$x10^{-6}$**
	α_1	**1.735**	

t (days)	ε_{cse} ($x10^{-6}$)	k_1	ε_{csd} ($x10^{-6}$)	ε_{cs} ($x10^{-6}$)
0	0	0.000	0	0
1	7	0.204	89	96
2	13	0.327	143	156
3	19	0.422	184	203
4	24	0.499	218	242
5	29	0.565	247	276
6	33	0.622	272	305
7	37	0.672	294	330
14	55	0.909	397	452
24	66	1.091	476	543
28	69	1.140	498	566
42	72	1.260	550	622
57	73	1.339	585	658
70	73	1.387	606	679
84	73	1.426	623	696
105	73	1.468	641	714
143	73	1.520	664	737
175	73	1.548	676	749
196	73	1.563	683	756
224	73	1.579	690	763
252	73	1.591	695	768
280	73	1.602	700	773
308	73	1.611	704	777
337	73	1.619	707	780
364	73	1.626	710	783

Shrinkage Prediction - Gilbert's Method		**(5DS)**	
Compressive strength (MPa)	**f'_c**	**27**	
Hypothetical thickness (mm)	**t_h**	**50**	
Interior environment	**k_4**	**0.65**	
Final endogenous shrinkage	**ε_{cse}***	**31**	
Quality of aggregate	**$\varepsilon_{csd.b*}$**	**1000**	**$x10^{-6}$, Perth**
Basic drying shrinkage	**$\varepsilon_{csd.b}$**	**784**	**$x10^{-6}$**
	α_1	**1.735**	

t (days)	**ε_{cse}**	**k_1**	**ε_{csd}**	**ε_{cs}**
	($x10^{-6}$)		**($x10^{-6}$)**	**($x10^{-6}$)**
0	0	0.000	0	0
1	3	0.204	104	107
2	6	0.327	167	172
3	8	0.422	215	223
4	10	0.499	254	265
5	12	0.565	288	300
6	14	0.622	317	331
7	16	0.672	342	358
14	23	0.909	463	487
24	28	1.091	556	584
28	29	1.140	581	610
42	31	1.260	642	672
57	31	1.339	682	713
70	31	1.387	707	738
84	31	1.426	727	758